Numerical Inversion of the Funk transform on the Rotation Group

Ralf Hielscher *

October 22, 2013

Abstract

The reconstruction of a function on the rotation group from mean values along all geodesics is an overdetermined problem, i.e., it is sufficient to know the mean values for a three dimensional subset of all geodesics on the rotation group. In this paper we give a Fourier slice theorem for the restricted problem. Based on the Fourier slice theorem and fast Fourier transforms on the rotation group and the sphere we introduce a fast algorithm for the forward transform. Analyzing the inverse problem we come up with an exact inversion formula for bandlimited functions on the rotation group. Unfortunately, this inversion formula turns out to be extremely ill conditioned. Therefore, we introduce an iterative approach which makes use of regularization and the fast algorithm for the forward transform. Numerical experiments indicate the applicability of our algorithms.

1 Introduction

The reconstruction of functions from mean values along certain submanifolds is a well studied problem within several fields of mathematics with numerous applications, most notably, in imaging. In this paper we consider the specific case that the function $f\colon \mathrm{SO}(3) \to \mathbb{R}$ to be recovered is defined on the rotation group $\mathrm{SO}(3)$ and the submanifolds are the geodesics on the rotation group. The family of all geodesics $C \subset \mathrm{SO}(3)$ on the rotation group may be parametrized by two unit vectors $\boldsymbol{\xi}, \boldsymbol{\eta} \in \mathbb{S}^2$ on the sphere $\mathbb{S}^2 = \{\, \boldsymbol{\xi} \in \mathbb{R}^3 \mid |\boldsymbol{\xi}| = 1 \,\}$ as

$$C(\boldsymbol{\xi}, \boldsymbol{\eta}) = \{\, \mathbf{R} \in \mathrm{SO}(3) \mid \mathbf{R}\boldsymbol{\xi} = \boldsymbol{\eta} \,\}.$$

Hence, we are interested in the inversion of the Funk transform

$$\mathcal{M}f(\boldsymbol{\xi}, \boldsymbol{\eta}) = \int_{C(\boldsymbol{\xi}, \boldsymbol{\eta})} f(\mathbf{R}) \,\mathrm{d}\mathbf{R},$$

*Chemnitz University of Technology

which assigns to a function $f\colon \mathrm{SO}(3) \to \mathbb{C}$ its mean values along all geodesics $C(\boldsymbol{\xi}, \boldsymbol{\eta})$, $\boldsymbol{\xi}, \boldsymbol{\eta} \in \mathbb{S}^2$.

One reason why we are interested in this particular manifold is that the inversion of the Funk transform on the rotation group is essential in quantitative texture analysis of polycrystalline materials by means of diffraction. There the alignment of a crystal within a polycrystalline material is described by a rotation that realizes the coordinate transform between a certain specimen fixed coordinate system and a crystal fixed coordinate system. Assigning a rotation to each crystal within the polycrystalline material one is interested in the distribution of these rotations. This distribution is modeled by a density function $f\colon \mathrm{SO}(3) \to \mathbb{R}_+$, the so called *orientation density function*. On the other hand diffraction measurements by X–ray, synchrotron or neutron diffraction results in point evaluations of the even part of the Funk transform

$$g(\boldsymbol{\xi}, \boldsymbol{\eta}) = \frac{1}{2}\big(\mathcal{M}f(\boldsymbol{\xi}, \boldsymbol{\eta}) + \mathcal{M}f(-\boldsymbol{\xi}, \boldsymbol{\eta})\big)$$

of the orientation density function, (cf. [5, 23]). Due to this practical importance there are a lot of papers by engineers and physicists on the inversion of the Funk transform, see e.g. [4, 31, 29, 32, 38, 13, 6, 28, 35, 22, 10, 37, 34, 43, 23, 1]. There are also a few mathematical papers on this topic covering quite different inversion methods, i.e., splines [40, 12, 3], Fourier expansion [11], Gabor frames [7] and wavelets [2]. However, those papers mainly focus on complete data, i.e., sampling sets $(\boldsymbol{\xi}_m, \boldsymbol{\eta}_{m'})$, $m, m' = 1, \ldots, M$, where $\boldsymbol{\xi}_m, \boldsymbol{\eta}_{m'}$, $m, m' = 1, \ldots, M$ are dense spherical grids.

The Funk transform can be seen in analogy to the X-ray transform where a function $f\colon \mathbb{R}^3 \to \mathbb{R}$ is associated with its integrals

$$\mathcal{X}f(\mathbf{x}, \mathbf{y}) = \int_{\mathbb{R}} f(\mathbf{x} + t(\mathbf{x} - \mathbf{y}))\,\mathrm{d}t, \quad \mathbf{x}, \mathbf{y} \in \mathbb{R}^3,$$

along straight lines. In both cases the central problem is the reconstruction of f from discrete samples of $\mathcal{M}f$ or $\mathcal{X}f$, respectively. In computed tomography it is a well known fact that the reconstruction of f does not require the means along all straight lines, but, it is already sufficient to know the means along all straight lines that are perpendicular to an arbitrarily fixed direction. This is due to the fact that the X-ray transform $g = \mathcal{X}f$ of f satisfies Johns equation (cf. [14])

$$\left(\frac{\partial}{\partial \mathbf{x}_i \partial \mathbf{y}_j} - \frac{\partial}{\partial \mathbf{x}_j \partial \mathbf{y}_i}\right) g = 0, \quad i, j = 1, 2, 3 \tag{1}$$

and the set Ω of all straight lines that are perpendicular to a certain direction forms a characteristic set, i.e., the condition $g|_\Omega = 0$ turns the ultrahyperbolic partial equation (1) into a well posed boundary value problem. It turns out that a similar ultrahyperbolic partial differential equation is satisfied by the Funk transform of a function on the rotation group [26]. This gives rise to the recent discovery of three dimensional characteristic sets Ω for the Funk transform $\mathcal{M}$ by Palamodov [27] which consist of all geodesics that intersect an arbitrarily fixed geodesics. In particular, he showed that the original function f can be inverted from data $\mathcal{M}f|_\Omega$ by inverting the spherical Funk transform on spherical sections of the rotation group. In his paper the continuous problem was considered, i.e., the inversion based on a discrete sampling set as well as fast inversion algorithms are still open problems.

In this paper we develop global Fourier based reconstruction algorithms for the Funk transform restricted to characteristic sets, i.e., we assume discrete data $\mathcal{M}f(\boldsymbol{\xi}_m, \boldsymbol{\eta}_m)$, $m = 1, \ldots, M$ given at nodes $(\boldsymbol{\xi}_m, \boldsymbol{\eta}_m) \in \Omega$, that belong to a characteristic subset $\Omega \subset \mathbb{S}^2 \times \mathbb{S}^2$ and aim at the recovery of the Fourier coefficients of f. The findings of our paper are as follows. In Theorem 7 we show that the restriction

$$\mathcal{M}\colon L^2(\mathrm{SO}(3)) \to L^2(\Omega)$$

of the Funk Transform to a characteristic set Ω is unbounded, while being bounded as an operator

$$\mathcal{M}\colon C(\mathrm{SO}(3)) \to C(\Omega).$$

For functions with absolutely convergent Fourier series we give in Theorem 8 a decomposition of the restricted Funk transform into a Fourier transform on the rotation group, a block diagonal operator with triangular blocks, a rotation operator in Fourier space and a Fourier transform on the tensor product space $\mathbb{S}^2 \otimes \mathbb{S}^1$. This decomposition can be seen as a specialization of the Fourier slice theorem for the Funk transform (cf. [11]) to the restricted case. A discrete version of this decomposition is given in Theorem 9.

As a direct application of our decomposition result we present a fast, approximate Algorithm 1 for the forward problem which has the numerical complexity $\mathcal{O}(N^{4/3})$ where N is the problem size, i.e. the number of sampling points as well as the number of Fourier coefficients used for the representation of the function f is of order $\mathcal{O}(N)$. To this end we utilized the nonequispaced fast Fourier transform on the sphere [17, 18] and the fast Fourier transform on the rotation group [20, 30, 19]. Numerical tests indicate the accuracy of our approximate algorithm.

Considering the inverse problem in Section 3.4 we present in Theorem 10 an exact discrete inversion formula for the restricted Funk transform of bandlimited functions. Unfortunately, this inversion formula turns out to be unstable as it is illustrated in Table 1. Therefore, we utilize the forward Algorithm 1 as well as the corresponding algorithm for the adjoined problem to implement an iterative solver for the normal equation. Following this approach we may apply regularization to our problem either in the form of oversampling or as Tychonov regularization. The numerical results presented in Figure 2 indicate that our algorithm may be suitable for practical applications.

2 Harmonic Analysis on the Rotation Group and the Sphere

2.1 Spherical harmonics

Let us denote by $\mathbf{e}_1 = (1,0,0)^T$, $\mathbf{e}_2 = (0,1,0)^T$, $\mathbf{e}_3 = (0,0,1)^T$ the canonical basis in $\mathbb{R}^3$ and by $\mathbb{S}^2 = \{\, \boldsymbol{\xi} \in \mathbb{R}^3 \mid |\boldsymbol{\xi}| = 1 \,\}$ the unit sphere. Then any vector $\mathbf{u}_{\theta,\rho} \in \mathbb{S}^2$ can be represented by its polar coordinates $(\theta, \rho) \in [0, \pi] \times [0, 2\pi)$,

$$\mathbf{u}_{\theta,\rho} = \cos\theta\, \mathbf{e}_3 + \sin\theta\, (\sin\rho\, \mathbf{e}_1 + \cos\rho\, \mathbf{e}_2)\,. \tag{2}$$

In terms of polar coordinate the spherical surface measure σ is given by

$$\int_{\mathbb{S}^2} f(\boldsymbol{\xi})\,\mathrm{d}\sigma(\boldsymbol{\xi}) = \int_0^{2\pi}\int_0^{\pi} f(\mathbf{u}_{\theta,\rho})\sin\theta\,\mathrm{d}\theta\,\mathrm{d}\rho$$

for any integrable function $f\colon \mathbb{S}^2 \to \mathbb{C}$. As usual we denote by $L^2(\mathbb{S}^2)$ the Hilbert space of square integrable functions on the sphere. An orthonormal basis in $L^2(\mathbb{S}^2)$ is formed by the well known spherical harmonics, cf. [25],

$$\mathcal{Y}_\ell^k(\mathbf{u}_{\theta,\rho}) = \sqrt{\frac{2\ell+1}{4\pi}}\mathcal{P}_\ell^{|k|}(\cos\theta)\mathrm{e}^{\mathrm{i}k\rho}, \quad \ell\in\mathbb{N}_0,\ k=-\ell,\dots,\ell, \tag{3}$$

with associated Legendre functions $\mathcal{P}_\ell^{|k|}$ defined in terms of the Legendre polynomials

$$\mathcal{P}_\ell(t) = \frac{1}{2^\ell \ell!}\frac{\mathrm{d}^\ell}{\mathrm{d}t^\ell}(t^2-1)^\ell, \quad t\in[-1,1],$$

by

$$\mathcal{P}_\ell^k(t) = \left(\frac{(\ell-k)!}{(\ell+k)!}\right)^{1/2}(1-t^2)^{k/2}\frac{\mathrm{d}^k}{\mathrm{d}t^k}\mathcal{P}_\ell(t).$$

Note, that we use associated Legendre functions normalized such that

$$\int_{\mathbb{S}^2}\mathcal{P}_\ell^k(\boldsymbol{\xi}\cdot\boldsymbol{\eta})^2\,\mathrm{d}\boldsymbol{\xi} = 2\pi\int_{-1}^1 \mathcal{P}_\ell^k(t)^2\,\mathrm{d}t = \frac{4\pi}{2\ell+1}, \quad \boldsymbol{\eta}\in\mathbb{S}^2 \tag{4}$$

and such that the Addition theorem [25] takes the form

$$\sum_{k=-\ell}^{\ell}\mathcal{Y}_\ell^k(\boldsymbol{\xi})\overline{\mathcal{Y}_\ell^k(\boldsymbol{\eta})} = \frac{2\ell+1}{4\pi}\mathcal{P}_\ell(\boldsymbol{\xi}\cdot\boldsymbol{\eta}).$$

In particular, we have by the Cauchy–Schwarz inequality the following upper bound on the spherical harmonics

$$\left|\mathcal{Y}_\ell^k(\boldsymbol{\xi})\right|^2 = \left|\frac{2\ell+1}{4\pi}\int_{\mathbb{S}^2}\mathcal{P}(\boldsymbol{\xi}\cdot\boldsymbol{\eta})\mathcal{Y}_\ell^k(\boldsymbol{\eta})\,\mathrm{d}\sigma(\boldsymbol{\eta})\right|^2 \le \frac{(2\ell+1)^2}{8\pi}\left\|\mathcal{Y}_\ell^k\right\|_2^2\left\|\mathcal{P}_\ell\right\|_2^2 = \frac{2\ell+1}{4\pi}.$$

The harmonic spaces $\mathrm{Harm}_\ell(\mathbb{S}^2) = \mathrm{span}\{\mathcal{Y}_\ell^{-\ell},\dots,\mathcal{Y}_\ell^\ell\}$, $\ell\in\mathbb{N}_0$, provide a complete system of rotational invariant, irreducible subspaces of $L^2(\mathbb{S}^2)$, i.e.,

$$L^2(\mathbb{S}^2) = \overline{\bigoplus_{\ell=0}^{\infty}\mathrm{Harm}_\ell(\mathbb{S}^2)}.$$

Let $L\in\mathbb{N}_0$. Then any function $f\in\Pi_L(\mathbb{S}^2) = \bigoplus_{\ell=0}^L \mathrm{Harm}_\ell(\mathbb{S}^2)$ is called spherical polynomial of degree L. For a given function $f\in L^2(\mathbb{S}^2)$ we define its Fourier sequence $\hat{f}\in\ell^2(I)$,

$$I = \{\,(\ell,k)\in\mathbb{Z}^2 \mid \ell\in\mathbb{N}_0,\ k=-\ell,\dots,\ell\,\},$$

as the sequence of coefficients with respect to the basis $\mathcal{Y}_\ell^k$, $(\ell,k) \in I$, i.e.,

$$\hat{f}(\ell,k) = \int_{\mathbb{S}^2} f(\boldsymbol{\xi})\overline{\mathcal{Y}_\ell^k(\boldsymbol{\xi})}\,\mathrm{d}\sigma(\boldsymbol{\xi}), \quad (\ell,k) \in I.$$

Moreover, we define the index set

$$I_L = \{\, (\ell,k) \in \mathbb{Z}^2 \mid \ell = 0,\ldots,L,\ k = -\ell,\ldots,\ell \,\},$$

of the Fourier coefficients of the space of spherical polynomials of degree $L \in \mathbb{N}_0$ which has the cardinality

$$|I_L| = (L+1)^2.$$

Definition 1. The *continuous Fourier transform* $\mathcal{F}_{\mathbb{S}^2}$ is the operator

$$\mathcal{F}_{\mathbb{S}^2} \colon \ell^2(I) \to L^2(\mathbb{S}^2), \quad \hat{f} \mapsto \sum_{(\ell,k)\in I} \hat{f}(\ell,k)\mathcal{Y}_\ell^k. \tag{5}$$

For a finite list of nodes $\boldsymbol{\xi}_m \in \mathbb{S}^2$, $m = 0,\ldots,M-1$ and a spherical polynomial f of degree L the *discrete Fourier transform* $\mathbf{F}_{L,\boldsymbol{\xi}} \colon \mathbb{C}^{I_L} \to \mathbb{C}^M$ is the operator defined by

$$[\mathbf{F}_{L,\boldsymbol{\xi}}\hat{\mathbf{f}}]_m = \sum_{(\ell,k)\in I_L} \hat{f}(\ell,k)\mathcal{Y}_\ell^k(\boldsymbol{\xi}_m), \quad m = 0,\ldots,M-1, \tag{6}$$

where $\hat{\mathbf{f}} \in \mathbb{C}^{I_L}$, $\hat{\mathbf{f}}_{\ell,k} = \hat{f}(\ell,k)$, $(\ell,k) \in I_L$ denotes the vector of Fourier coefficients of f.

By Parseval's theorem the operators $\mathcal{F}_{\mathbb{S}^2}$ and $\mathcal{F}_{\mathbb{S}^2}^{-1}$ are well defined isometries between $L^2(\mathbb{S}^2)$ and $\ell^2(I)$ and we have for any function $f \in L^2(\mathbb{S}^2)$

$$\mathcal{F}_{\mathbb{S}^2}^{-1} f = \hat{f}.$$

Unlike the Fourier transform on the torus the adjoined discrete Fourier transform on the sphere $\mathbf{F}_{L,\boldsymbol{\xi}}^H$ is in general not the inverse of $\mathbf{F}_{L,\boldsymbol{\xi}}$. In order to recover Fourier coefficients $\hat{f}(\ell,k)$, $(\ell,k) \in I_L$ we consider quadrature nodes $\boldsymbol{\xi}_m \in \mathbb{S}^2$, $m = 1,\ldots,M$ and corresponding quadrature weights ω_m such that

$$\hat{f}(\ell,k) = \sum_{m=1}^{M} \omega_m f(\boldsymbol{\xi}_m)\overline{\mathcal{Y}_\ell^k(\xi_m)}, \quad (\ell,k) \in I_L.$$

This sum may also written as an adjoined discrete spherical Fourier transform

$$\hat{\mathbf{f}} = \mathbf{F}_{L,\boldsymbol{\xi}}^H \mathbf{W}\mathbf{f},$$

where $\mathbf{f} = (f(\boldsymbol{\xi}_1),\ldots,f(\boldsymbol{\xi}_m))^T$ and $\mathbf{W} \in \mathbb{R}^{M\times M}$ is the diagonal matrix with entries $W_{m,m} = \omega_m$.

As an example of a spherical quadrature formula we consider for a maximum polynomial degree $L \in \mathbb{N}$ Clenshaw – Curtis quadrature nodes $\boldsymbol{\xi}_{m,n} = \mathbf{u}_{\rho_m,\theta_n}$, $m = 0,\ldots,2L+1$, $n = 0,\ldots,2L$ with

$$\rho_m = \frac{m\pi}{L+1}, \quad \theta_n = \frac{n\pi}{2L} \tag{7}$$

and the corresponding weights

$$\omega_n = \omega_{2L-n} = \left(\frac{4\pi\varepsilon_n^{2L}}{L(2L+2)} \sum_{\ell=0}^{L} \varepsilon_\ell^L \frac{1}{1-4\ell^2} \cos\frac{n\ell\pi}{L} \right)^2, \tag{8}$$

where

$$\varepsilon_n^L = \begin{cases} \frac{1}{2}, & \text{if } n=0 \text{ or } n=L, \\ 1, & \text{if } 0<n<L. \end{cases}$$

These weights can be computed efficiently by a discrete cosine transform or a fast Fourier transform (see e.g. [42]) and allow for the exact reconstruction of polynomials up to degree L.

2.2 Wigner-D functions

In this section we briefly recapitulate harmonic analysis on the rotation group. By the rotation group $\mathrm{SO}(3)$ we denote the set of all orthogonal, three by three matrices with determinant one. Any such matrix $\mathbf{R} \in \mathrm{SO}(3)$ can be interpreted as a rotation in the three dimensional Euclidean space about a certain axis of rotation $\boldsymbol{\xi} \in \mathbb{S}^2$ and a certain rotational angle $\omega = \omega(\mathbf{R}) = \arccos\frac{1}{2}(\operatorname{Tr}\mathbf{R} - 1)$, where $\operatorname{Tr}\mathbf{R}$ denotes the trace of $\mathbf{R}$. Conversely, we denote for every unit vector $\boldsymbol{\xi} \in \mathbb{S}^2$ and every angle $\omega \in [0, 2\pi)$ the matrix that acts as a rotation about ξ with angle ω by $\mathbf{R}_{\boldsymbol{\xi},\omega} \in \mathrm{SO}(3)$.

Since, $\mathrm{SO}(3)$ is a compact topological group it possesses a unique Haar measure λ such that $\lambda(\mathrm{SO}(3)) = 1$. Accordingly, we define the Hilbert space $L^2(\mathrm{SO}(3))$ as the space of square integrable functions on the rotation group endowed with the inner product

$$\langle f_1, f_2 \rangle = \int_{\mathrm{SO}(3)} f_1(\mathbf{R})\overline{f_2(\mathbf{R})}\,\mathrm{d}\lambda(\mathbf{R}), \quad f_1, f_2 \in L^2(\mathrm{SO}(3)),$$

and the corresponding norm $\|f\|_2 = \sqrt{\langle f, f\rangle}$. Setting

$$J = \{\, (\ell, k, k') \in \mathbb{Z}^3 \mid \ell \in \mathbb{N}_0,\ k, k' = -\ell, \ldots, \ell \,\},$$

we consider a system of harmonic functions on $\mathrm{SO}(3)$, called *Wigner–D functions* (cf. [41]),

$$D_\ell^{kk'}(\mathbf{R}) = \int_{\mathbb{S}^2} \mathcal{Y}_\ell^{k'}(\mathbf{R}^{-1}\boldsymbol{\xi})\overline{\mathcal{Y}_\ell^{k}(\boldsymbol{\xi})}\,\mathrm{d}\sigma(\boldsymbol{\xi}), \quad (\ell, k, k') \in J,\ \mathbf{R} \in \mathrm{SO}(3). \tag{9}$$

The Wigner–D functions are normalized such that $\|D_\ell^{kk'}\|^2 = \frac{8\pi^2}{2\ell+1}$ and form an orthogonal basis in $L^2(\mathrm{SO}(3))$. In particular, every function $f \in L^2(\mathrm{SO}(3))$ has a unique series expansion in terms of Wigner–D functions

$$f = \sum_{(\ell,k,k') \in J} \sqrt{\frac{2\ell+1}{8\pi^2}}\,\hat{f}(\ell, k, k') D_\ell^{kk'}, \tag{10}$$

with Fourier coefficients $\hat{f}(\ell,k,k')$, $(\ell,k,k') \in J$, given by the integrals

$$\hat{f}(\ell,k,k') = \sqrt{\frac{2\ell+1}{8\pi^2}} \int_{\mathrm{SO}(3)} f(\mathbf{R}) \overline{D_\ell^{kk'}(\mathbf{R})} \,\mathrm{d}\lambda(\mathbf{R}).$$

Let $\ell \in \mathbb{N}_0$. Then the *harmonic space* $\mathrm{Harm}_\ell(\mathrm{SO}(3))$ of degree ℓ is defined as

$$\mathrm{Harm}_\ell(\mathrm{SO}(3)) = \mathrm{span}_{k,k'=-\ell,\dots,\ell}\, D_\ell^{kk'}.$$

For reasons of analogy we call any function $f \in \Pi_L(\mathrm{SO}(3)) = \bigoplus_{\ell=0}^{L} \mathrm{Harm}_\ell(\mathrm{SO}(3))$ a *polynomial* on $\mathrm{SO}(3)$ of degree $L \in \mathbb{N}_0$ and correspondingly define the truncated index set

$$J_L = \{\, (\ell,k,k') \in \mathbb{Z}^3 \mid \ell = 0,\dots,L,\ k,k' = -\ell,\dots,\ell \,\}.$$

The dimension of the space of these polynomials is given by

$$|J_L| = \frac{1}{3}(L+1)(2L+1)(2L+3).$$

Similar to the spherical case we introduce the Fourier transform in $L^2(\mathrm{SO}(3))$.

Definition 2. The *continuous Fourier transform* on $\mathrm{SO}(3)$ is the operator

$$\mathcal{F}_{\mathrm{SO}(3)} \colon \ell^2(J) \to L^2(\mathrm{SO}(3)), \quad \hat{f} \mapsto \sum_{(\ell,k,k') \in J} \sqrt{\frac{2\ell+1}{8\pi^2}} \hat{f}(\ell,k,k') D_\ell^{kk'}. \tag{11}$$

For a finite list of rotations $\mathbf{R}_m \in \mathrm{SO}(3)$, $m = 0,\dots,M-1$ and a polynomial $f \in \Pi_L(\mathrm{SO}(3))$ of degree L the *discrete Fourier transform* $\mathbf{F}_{L,\mathbf{R}} \colon \mathbb{C}^{J_L} \to \mathbb{C}^M$ is the operator

$$[\mathbf{F}_{L,\mathbf{R}} \hat{\mathbf{f}}]_m = \sum_{(\ell,k,k') \in J_L} \sqrt{\frac{2\ell+1}{8\pi^2}} \hat{f}(\ell,k,k') D_\ell^{kk'}(\mathbf{R}_m), \quad m = 0,\dots,M-1 \tag{12}$$

where $\hat{\mathbf{f}} \in \mathbb{C}^{J_L}$, $\hat{\mathbf{f}}_{\ell,k,k'} = \hat{f}(\ell,k,k)$, $(\ell,k,k') \in J_L$ denotes the vector of Fourier coefficients of f.

By Parseval's theorem the operators $\mathcal{F}_{\mathrm{SO}(3)}$, $\mathcal{F}_{\mathrm{SO}(3)}^{-1}$ are well defined isometries between $L^2(\mathrm{SO}(3))$ and $\ell^2(J)$ and we have for any function $f \in L^2(\mathrm{SO}(3))$

$$\mathcal{F}_{\mathrm{SO}(3)}^{-1} f = \hat{f}.$$

3 The Funk Transform on the Rotation Group

3.1 Basic properties

Let $\boldsymbol{\xi}, \boldsymbol{\eta} \in \mathbb{S}^2$ be two unit vectors, let $\mathbf{R}_0 \in \mathrm{SO}(3)$ be an arbitrary rotation with $\mathbf{R}_0 \boldsymbol{\xi} = \boldsymbol{\eta}$ and remember that $\mathbf{R}_{\boldsymbol{\eta},\omega}$ denotes a rotation with rotational axis $\boldsymbol{\eta}$ and angle $\omega \in [0, 2\pi)$. Then the set

$$C(\boldsymbol{\xi},\boldsymbol{\eta}) = \{\, \mathbf{R} \in \mathrm{SO}(3) \mid \mathbf{R}\boldsymbol{\xi} = \boldsymbol{\eta} \,\} = \{\, \mathbf{R}_{\boldsymbol{\eta},\omega} \mathbf{R}_0 \mid \omega \in [0,2\pi) \,\}$$

of all rotations $\mathbf{R} \in \mathrm{SO}(3)$ that map $\boldsymbol{\xi}$ onto $\boldsymbol{\eta}$ is a geodesics in $\mathrm{SO}(3)$. Furthermore, $C(\boldsymbol{\xi},\boldsymbol{\eta}) = C(-\boldsymbol{\xi},-\boldsymbol{\eta})$, $\boldsymbol{\xi},\boldsymbol{\eta} \in \mathbb{S}^2$ is a parametrization of all geodesics in $\mathrm{SO}(3)$, cf. [24].

Definition 3. The Funk transform on the rotation group is the operator

$$\begin{aligned}&\mathcal{M}\colon L^2(\mathrm{SO}(3)) \to L^2(\mathbb{S}^2 \times \mathbb{S}^2),\\ &\mathcal{M}f(\boldsymbol{\xi},\boldsymbol{\eta}) = \frac{1}{2\pi}\int_{C(\boldsymbol{\xi},\boldsymbol{\eta})} f(\mathbf{R})\,\mathrm{d}\mathbf{R} = \frac{1}{2\pi}\int_0^{2\pi} f(\mathbf{R}_{\boldsymbol{\eta},\omega}\mathbf{R}_0)\,\mathrm{d}\omega\end{aligned}$$

that assign to a function $f\colon \mathrm{SO}(3) \to \mathbb{R}$ its means along all geodesics.

The operator $\mathcal{M}$ is sometimes also called *Radon transform*, cf. [9]. For f being a Wigner-D function its Funk transform is known explicitly (cf. [40]).

Lemma 4. *The Funk transform of the Wigner–D functions $D_\ell^{kk'}$, $(\ell,k,k') \in J$ is given by*

$$\mathcal{M}D_\ell^{kk'}(\boldsymbol{\xi},\boldsymbol{\eta}) = \frac{4\pi}{2\ell+1}\mathcal{Y}_\ell^{k'}(\boldsymbol{\xi})\overline{\mathcal{Y}_\ell^{k}(\boldsymbol{\eta})}, \quad \boldsymbol{\xi},\boldsymbol{\eta} \in \mathbb{S}^2.$$

As a consequence the range of the Funk transform can be characterized as a closed subspace of the Sobolev space $\mathcal{H}_{\frac{1}{2}}(\mathbb{S}^2 \times \mathbb{S}^2)$ of functions

$$g(\boldsymbol{\xi},\boldsymbol{\eta}) = \sum_{(\ell,k)\in I}\sum_{(\tilde{\ell},\tilde{k})\in I} \hat{g}(\ell,k,\tilde{\ell},\tilde{k})\mathcal{Y}_\ell^k(\boldsymbol{\xi})\mathcal{Y}_{\tilde{\ell}}^{\tilde{k}}(\boldsymbol{\eta})$$

with Fourier coefficients satisfying

$$\sum_{(\ell,k)\in I}\sum_{(\tilde{\ell},\tilde{k})\in I} (1+\ell^2+\tilde{\ell}^2)\left|\hat{g}(\ell,k,\tilde{\ell},\tilde{k})\right|^2 \leq \infty.$$

More precisely, one can find in [40] the following result.

Theorem 5. *The Funk transform $\mathcal{M}\colon L^2(\mathrm{SO}(3)) \to \mathcal{H}_{1/2}(\mathbb{S}^2 \times \mathbb{S}^2)$ defines an injective, open and bounded operator. Its range is characterized by the ultrahyperbolic partial differential equation*

$$(\triangle_{\boldsymbol{\xi}} - \triangle_{\boldsymbol{\eta}})\mathcal{M}f(\boldsymbol{\xi},\boldsymbol{\eta}) = 0, \quad \boldsymbol{\xi},\boldsymbol{\eta} \in \mathbb{S}^2, \tag{13}$$

where $\triangle_{\boldsymbol{\xi}}$ and $\triangle_{\boldsymbol{\eta}}$ are the spherical Laplace Beltrami operators with respect to the first and the second variable, respectively.

3.2 The restricted Funk transform

Assume $\Omega \subset \mathbb{S}^2 \times \mathbb{S}^2$ to be a three dimensional subset such that the boundary value problem

$$(\triangle_{\boldsymbol{\xi}} - \triangle_{\boldsymbol{\eta}})g(\boldsymbol{\xi},\boldsymbol{\eta}) = 0, \quad g|_\Omega = 0$$

has a unique solution g. Then we call Ω a characteristic set for the partial differential equation (13) and according to Theorem 5 the restriction $\mathcal{M}|_\Omega$ of the Funk transform to Ω is invertible.

Characteristic sets for the Funk transform on the rotation group where found recently by Palamodov [27]. Let $C(\boldsymbol{\xi}_0, \boldsymbol{\eta}_0) \subset \mathrm{SO}(3)$, $\boldsymbol{\xi}_0, \boldsymbol{\eta}_0 \in \mathbb{S}^2$ be a geodesics in $\mathrm{SO}(3)$. Then the subset

$$\Omega_{\boldsymbol{\xi}_0,\boldsymbol{\eta}_0} = \{\, (\boldsymbol{\xi}, \boldsymbol{\eta}) \in \mathbb{S}^2 \times \mathbb{S}^2 \mid C(\boldsymbol{\xi}_0, \boldsymbol{\eta}_0) \cap C(\boldsymbol{\xi}, \boldsymbol{\eta}) \neq \emptyset \,\} \subset \mathbb{S}^2 \times \mathbb{S}^2$$

which consists of all geodesics intersecting $C(\boldsymbol{\xi}_0, \boldsymbol{\eta}_0)$ is a characteristic subset. For the remainder of this paper we restrict ourselves to the set $\Omega_{\mathbf{e}_3,\mathbf{e}_3}$ as any other set $\Omega_{\boldsymbol{\xi}_0,\boldsymbol{\eta}_0}$ is just a rotated version of it. More precisely, we have the following lemma.

Lemma 6. *Let $\boldsymbol{\xi}_0, \boldsymbol{\eta}_0 \in \mathbb{S}^2$. Then*

$$\Omega_{\boldsymbol{\xi}_0,\boldsymbol{\eta}_0} = \{\, (\boldsymbol{\xi}, \boldsymbol{\eta}) \in \mathbb{S}^2 \times \mathbb{S}^2 \mid \boldsymbol{\xi} \cdot \boldsymbol{\xi}_0 = \boldsymbol{\eta} \cdot \boldsymbol{\eta}_0 \,\}. \tag{14}$$

Let, furthermore, $\mathbf{L}, \mathbf{R} \in \mathrm{SO}(3)$ such that $\mathbf{L}\mathbf{e}_3 = \boldsymbol{\xi}_0$ and $\mathbf{R}\mathbf{e}_3 = \boldsymbol{\eta}_0$. Then $(\boldsymbol{\xi}, \boldsymbol{\eta}) \in \Omega_{\mathbf{e}_3,\mathbf{e}_3}$ if and only if $(\mathbf{L}\boldsymbol{\xi}, \mathbf{R}\boldsymbol{\eta}) \in \Omega_{\boldsymbol{\xi}_0,\boldsymbol{\eta}_0}$. With the translation operator

$$T_{\mathbf{L},\mathbf{R}} \colon L^2(\mathrm{SO}(3)) \to L^2(\mathrm{SO}(3)), \quad T_{\mathbf{L},\mathbf{R}} f(\mathbf{A}) = f(\mathbf{L}\mathbf{A}\mathbf{R}^{-1}), \quad \mathbf{A} \in \mathrm{SO}(3)$$

we have

$$\mathcal{M}\, T_{\mathbf{L},\mathbf{R}} f(\boldsymbol{\xi}, \boldsymbol{\eta}) = \mathcal{M} f(\mathbf{R}\boldsymbol{\xi}, \mathbf{L}\boldsymbol{\eta}), \quad (\boldsymbol{\xi}, \boldsymbol{\eta}) \in \Omega_{\mathbf{e}_3,\mathbf{e}_3}.$$

Proof. Let $\boldsymbol{\xi}_0, \boldsymbol{\eta}_0, \boldsymbol{\xi}, \boldsymbol{\eta} \in \mathbb{S}^2$. Then the geodesics $C(\boldsymbol{\xi}_0, \boldsymbol{\eta}_0)$ and $C(\boldsymbol{\xi}, \boldsymbol{\eta})$ have a common rotation if there is a rotation $\mathbf{R} \in \mathrm{SO}(3)$ with $\mathbf{R}\boldsymbol{\xi}_0 = \boldsymbol{\eta}_0$ and $\mathbf{R}\boldsymbol{\xi} = \boldsymbol{\eta}$, i.e., if and only if $\boldsymbol{\xi}_0 \cdot \boldsymbol{\xi} = \boldsymbol{\eta}_0 \cdot \boldsymbol{\eta}$. This proves (14).

As for the action of the translation operator $T_{\mathbf{L},\mathbf{R}}$, simple calculations yield

$$\mathcal{M} T_{\mathbf{L},\mathbf{R}} f(\boldsymbol{\xi}, \boldsymbol{\eta}) = \frac{1}{2\pi} \int_{\mathbf{A}\boldsymbol{\xi}=\boldsymbol{\eta}} f(\mathbf{L}\mathbf{A}\mathbf{R}^{-1}) \,\mathrm{d}\mathbf{A} = \frac{1}{2\pi} \int_{\tilde{\mathbf{A}}\mathbf{R}\boldsymbol{\xi}=\mathbf{L}\boldsymbol{\eta}} f(\tilde{\mathbf{A}}) \,\mathrm{d}\tilde{\mathbf{A}} = \mathcal{M} f(\mathbf{R}\boldsymbol{\xi}, \mathbf{L}\boldsymbol{\eta}).$$

□

The characteristic subset $\Omega_{\mathbf{e}_3,\mathbf{e}_3}$ is a differentiable submanifold of $\mathbb{S}^2 \times \mathbb{S}^2$ except for the singular point $(\mathbf{e}_3, \mathbf{e}_3)$. The induced measure with respect to the polar coordinates $(\theta, \rho, \rho') \mapsto (\mathbf{u}_{\theta,\rho}, \mathbf{u}_{\theta,\rho'}) \in \Omega_{\mathbf{e}_3,\mathbf{e}_3}$, cf. (2), is given by

$$\int_{\Omega_{\mathbf{e}_3,\mathbf{e}_3}} f(\boldsymbol{\xi}, \boldsymbol{\eta}) \,\mathrm{d}(\boldsymbol{\xi}, \boldsymbol{\eta}) = \int_0^{\pi} \int_0^{2\pi} \int_0^{2\pi} f(\mathbf{u}_{\theta,\rho}, \mathbf{u}_{\theta,\rho'}) \sin^2\theta \,\mathrm{d}\rho \,\mathrm{d}\rho' \,\mathrm{d}\theta$$

and allows us to introduce the space $L^2(\Omega_{\mathbf{e}_3,\mathbf{e}_3})$ of square integrable functions on this specific domain. Unfortunately, the restricted Funk transform is unbounded in the L^2 setting.

Theorem 7. *The restriction of the Funk transform on the rotation group to $\Omega_{\mathbf{e}_3,\mathbf{e}_3}$,*

$$\mathcal{M}|_{\Omega_{\mathbf{e}_3,\mathbf{e}_3}} \colon L^2(\mathrm{SO}(3)) \to L^2(\Omega_{\mathbf{e}_3,\mathbf{e}_3})$$

is an unbounded operator, while being bounded as the operator

$$\mathcal{M}|_{\Omega_{\mathbf{e}_3,\mathbf{e}_3}} \colon C(\mathrm{SO}(3)) \to C(\Omega_{\mathbf{e}_3,\mathbf{e}_3}).$$

Proof. For $n > 0$ we consider the function

$$f(\mathbf{R}) = F(\mathbf{R}\mathbf{e}_3 \cdot \mathbf{e}_3) = (1 - \mathbf{R}\mathbf{e}_3 \cdot \mathbf{e}_3)^{\frac{1}{n}-\frac{1}{2}}.$$

Using the Euler angle parameterization $\mathbf{R} = \mathbf{R}_{\mathbf{e}_3,\phi_1}\mathbf{R}_{\mathbf{e}_2,\Phi}\mathbf{R}_{\mathbf{e}_3,\phi_2}$ we obtain for the L^2–norm

$$\begin{aligned}\int_{\mathrm{SO}(3)} f(\mathbf{R})^2 \,\mathrm{d}\mathbf{R} &= \int_0^{2\pi}\int_0^{\pi}\int_0^{2\pi} F(\mathbf{R}_{\mathbf{e}_3,\phi_1}\mathbf{R}_{\mathbf{e}_2,\Phi}\mathbf{R}_{\mathbf{e}_3,\phi_2}\mathbf{e}_3 \cdot \mathbf{e}_3)^2 \sin\Phi \,\mathrm{d}\phi_1\,\mathrm{d}\Phi\,\mathrm{d}\phi_2 \\ &= 4\pi^2 \int_0^{\pi} (1-\cos\Phi)^{\frac{2}{n}-1} \sin\Phi\,\mathrm{d}\Phi = 2^{1+\frac{2}{n}}\pi^2 n. \qquad (15)\end{aligned}$$

For $(\boldsymbol{\xi}, \boldsymbol{\eta}) \in \Omega_{\mathbf{e}_3,\mathbf{e}_3}$ and $\boldsymbol{\xi} \cdot \mathbf{e}_3 = \boldsymbol{\eta} \cdot \mathbf{e}_3 = \cos\theta$ the Funk transform of f computes to

$$\mathcal{M}f(\boldsymbol{\xi}, \boldsymbol{\eta}) = \frac{1}{2\pi}\int_0^{2\pi} F(\cos^2\theta + \sin^2\theta\cos\omega)\,\mathrm{d}\omega.$$

Substituting $t = \cos^2\theta + \sin^2\theta\cos\omega$ and observing that

$$\sin^2\omega = 1 - \left(\frac{t-\cos^2\theta}{\sin^2\theta}\right)^2 = \frac{(1-t)(t-\cos 2\theta)}{\sin^4\theta}$$

and

$$\mathrm{d}t = -\sin^2\theta\sin\omega\,\mathrm{d}\omega = -\sqrt{(1-t)(t-\cos 2\theta)}\,\mathrm{d}\omega$$

we obtain

$$\mathcal{M}f(\boldsymbol{\xi}, \boldsymbol{\eta}) = \int_{\cos 2\theta}^{1} \frac{(1-t)^{\frac{1}{n}-\frac{1}{2}}}{\sqrt{1-t}\sqrt{t-\cos 2\theta}}\,\mathrm{d}t \geq \frac{1}{2}\int_{\cos 2\theta}^{1} (1-t)^{\frac{1}{n}-1}\,\mathrm{d}t = (1-\cos 2\theta)^{\frac{1}{n}} n.$$

Consequently,

$$\int_{\Omega_{\mathbf{e}_3,\mathbf{e}_3}} |\mathcal{M}f(\boldsymbol{\xi}, \boldsymbol{\eta})|^2 \,\mathrm{d}(\boldsymbol{\xi}, \boldsymbol{\eta}) = 4\pi^2 n^2 \int_0^{\pi} (1-\cos 2\theta)^{\frac{2}{n}} \sin^2\theta\,\mathrm{d}\theta \geq Cn^2. \qquad (16)$$

By comparing (15) and (16) for $n \to \infty$ we conclude that the restricted Funk transform is unbounded.

The fact that the restricted Funk transform is bounded with respect to maximum norm follows from the estimate

$$|\mathcal{M}f(\boldsymbol{\xi}, \boldsymbol{\eta})| \leq \frac{1}{2\pi}\int_{C(\boldsymbol{\xi},\boldsymbol{\eta})} |f(\mathbf{R})|\,\mathrm{d}\mathbf{R} \leq \max_{\mathbf{R}\in\mathrm{SO}(3)} |f(\mathbf{R})|, \quad \boldsymbol{\xi}, \boldsymbol{\eta} \in \mathbb{S}^2.$$

□

For the unrestricted Funk transform a Fourier slice theorem based on Lemma 4 is known (cf. [11]) and is effectively used for its inversion. Our next goal is to derive a similar result for the restricted Funk transform $\mathcal{M}|_{\Omega_{\mathbf{e}_3,\mathbf{e}_3}}$. The corner stone for our approach is the fact that the product of two spherical polynomials of degree L is again a spherical polynomial of degree $2L$. The Fourier coefficients of the product are related to the Fourier coefficients of the factors by the so called connection coefficients or Clebsch – Gordan coefficients $\langle j_1\ m_1\ j_2\ m_2 \mid J\ M\rangle$ (cf. [39]). More precisely, we have

$$Y_\ell^k(\boldsymbol{\xi})Y_\ell^{k'}(\boldsymbol{\xi}) = \frac{2\ell+1}{\sqrt{4\pi}} \sum_{\lambda=\left\lceil\frac{|k+k'|}{2}\right\rceil}^{\ell} \frac{1}{\sqrt{4\lambda+1}} \langle \ell\ 0\ \ell\ 0 \mid 2\lambda\ 0\rangle \langle \ell\ k\ \ell\ k' \mid 2\lambda\ k+k'\rangle\, Y_{2\lambda}^{k+k'}(\boldsymbol{\xi}), \tag{17}$$

where $\lceil x \rceil$ denotes the smallest integer that is larger or equal to x. With

$$\mathcal{Y}_\ell^k(\mathbf{u}_{\theta,\rho}) = \sqrt{\frac{2\ell+1}{4\pi}}\mathrm{e}^{\mathrm{i}k\rho}P_\ell^{|k|}(\cos\theta) \text{ and } C_{\ell k k'}^{\lambda} = \langle \ell\ 0\ \ell\ 0 \mid \lambda\ 0\rangle \langle \ell\ k\ \ell\ k' \mid \lambda\ k+k'\rangle$$

the above equality can be restated for products of associated Legendre functions as

$$\begin{aligned}
P_\ell^{|k|}(\cos\theta)P_\ell^{|k'|}(\cos\theta) &= \sum_{\lambda=\left\lceil\frac{|k+k'|}{2}\right\rceil}^{\ell} \langle \ell\ 0\ \ell\ 0 \mid 2\lambda\ 0\rangle \langle \ell\ k\ \ell\ k' \mid 2\lambda\ k+k'\rangle\, P_{2\lambda}^{|k+k'|}(\cos\theta) \\
&= \sum_{\lambda=\left\lceil\frac{|k+k'|}{2}\right\rceil}^{\ell} C_{\ell k k'}^{2\lambda} P_{2\lambda}^{|k+k'|}(\cos\theta)
\end{aligned}$$

and, hence, we have for arbitrary vectors $\mathbf{u}_{\theta,\rho}, \mathbf{u}_{\theta,\rho'} \in \mathbb{S}^2$ with the same distance $\theta \in [0,\pi]$ to $\mathbf{e}_3$ the expansion

$$Y_\ell^{k'}(\mathbf{u}_{\theta,\rho})\overline{Y_\ell^k(\mathbf{u}_{\theta,\rho'})} = \frac{2\ell+1}{4\pi} \sum_{\lambda=\left\lceil\frac{|k+k'|}{2}\right\rceil}^{\ell} C_{\ell k k'}^{2\lambda} P_{2\lambda}^{|k+k'|}(\cos\theta)\mathrm{e}^{\mathrm{i}('k\rho - k\rho')}. \tag{18}$$

Let $f \in L^2(\mathrm{SO}(3))$ with Fourier coefficients $\hat{f}(\ell,k,k')$, $(\ell,k,k') \in J$, cf. (10). According to Lemma 4 its Funk transforms $\mathcal{M}f(\mathbf{u}_{\theta,\rho},\mathbf{u}_{\theta,\rho'})$ can be written as a series of products of spherical harmonics. Applying the polynomial transform (18) we obtain

$$\begin{aligned}
\mathcal{M}f(\mathbf{u}_{\theta,\rho},\mathbf{u}_{\theta,\rho'}) &= \sum_{(\ell,k,k')\in J} \sqrt{\frac{2}{2\ell+1}}\hat{f}(\ell,k,k')Y_\ell^{k'}(\mathbf{u}_{\theta,\rho})\overline{Y_\ell^k(\mathbf{u}_{\theta,\rho'})} \\
&= \sum_{(\ell,k,k')\in J} \sqrt{\frac{2\ell+1}{8\pi^2}} \sum_{\lambda=\left\lceil\frac{|k+k'|}{2}\right\rceil}^{\ell} \hat{f}(\ell,k,k')C_{\ell k k'}^{2\lambda} P_{2\lambda}^{|k+k'|}(\cos\theta)\mathrm{e}^{\mathrm{i}(k'\rho - k\rho')}.
\end{aligned} \tag{19}$$

The idea is to interchange the sums in (19). To this end we define the index set

$$\tilde{J} = \{\, (2\lambda,k,k') \in 2\mathbb{N}_0 \times \mathbb{Z} \times \mathbb{Z} \mid |k+k'| \le 2\lambda \,\}$$

and the following operators which eventually will give the decomposition of the restricted Funk transform.

1. An unbounded block diagonal operator $\mathcal{C}\colon \ell^2(J) \to \ell^2(\tilde{J})$,

$$\mathcal{C}\hat{f}(2\lambda, k, k') = \sum_{\ell=\lambda}^{L} \frac{\sqrt{2\ell+1}}{\sqrt{4\lambda+1}} C_{\ell k k'}^{2\lambda} \hat{f}(\ell, k, k'), \quad (2\lambda, k, k') \in \tilde{J},$$

with domain of definition $D(\mathcal{C}) = \{\, \hat{f} \in \ell^2(J) \mid \mathcal{C}\hat{f} \in \ell^2(\tilde{J}) \,\}$.

2. A rotation operator in Fourier space $\mathcal{P}\colon \ell^2(\tilde{J}) \to \ell^2(I \times \mathbb{Z})$,

$$\mathcal{P}\hat{h}(\lambda, k_+, k_-) = \begin{cases} \hat{h}(\lambda, \frac{k_++k_-}{2}, \frac{k_+-k_-}{2}), & (\lambda, \frac{k_++k_-}{2}, \frac{k_+-k_-}{2}) \in \tilde{J} \\ 0, & \text{otherwise} \end{cases}, \quad (\lambda, k_+) \in I, k_- \in \mathbb{Z}, \tag{20}$$

3. The tensor product Fourier transform $\mathcal{F}_{\mathbb{S}^2} \hat{\otimes} \mathcal{F}_{\mathbb{S}^1} : \ell^2(I \times \mathbb{Z}) \to L^2(\mathbb{S}^2 \times \mathbb{S}^1)$,

$$\mathcal{F}_{\mathbb{S}^1} \hat{\otimes} \mathcal{F}_{\mathbb{S}^2} \hat{g}(\boldsymbol{\xi}, \mathbf{u}_\rho) = \frac{1}{\sqrt{2\pi}} \sum_{(\lambda, k_+) \in I} \sum_{k_- \in \mathbb{Z}} \hat{g}(\lambda, k_+, k_-) \mathcal{Y}_\lambda^{k_+}(\boldsymbol{\xi}) \mathrm{e}^{\mathrm{i}k_-\rho},$$

where we have used the abbreviation $\mathbf{u}_\rho = (\cos\rho, \sin\rho)^T$ to denote vectors $\mathbf{u}_\rho \in \mathbb{S}^1$.

Theorem 8. *Let $f \in L^2(\mathrm{SO}(3))$ such that its Fourier coefficients $\hat{f} \in \ell_1(J)$ are absolutely summable. Then for a point $(\mathbf{u}_{\theta,\rho}, \mathbf{u}_{\theta,\rho'}) \in \Omega_{\mathbf{e}_3,\mathbf{e}_3}$ of the characteristic subset and a corresponding vector $(\mathbf{u}_{\theta,\frac{\rho+\rho'}{2}}, \mathbf{u}_{\frac{\rho-\rho'}{2}}) \in \mathbb{S}^2 \times \mathbb{S}^1$ the restriction $\mathcal{M}|_{\Omega_{\mathbf{e}_3,\mathbf{e}_3}}$ of the Funk transform to the characteristic set $\Omega_{\mathbf{e}_3,\mathbf{e}_3}$ allows for the decomposition*

$$\mathcal{M}f(\mathbf{u}_{\theta,\rho}, \mathbf{u}_{\theta,\rho'}) = \left(\mathcal{F}_{\mathbb{S}^2} \hat{\otimes} \mathcal{F}_{\mathbb{S}^1} \, \mathcal{P} \, \mathcal{C} \, \mathcal{F}_{\mathrm{SO}(3)}^{-1} f \right) (\mathbf{u}_{\theta,\frac{\rho+\rho'}{2}}, \mathbf{u}_{\frac{\rho-\rho'}{2}}). \tag{21}$$

Proof. Since we assumed the Fourier coefficients of f to be absolutely summable. The Fourier series of its Funk transform is absolutely convergent and we have by (19),

$$\mathcal{M}f(\mathbf{u}_{\theta,\rho}, \mathbf{u}_{\theta,\rho'}) = \sum_{(\ell,k,k') \in J} \sqrt{\frac{2\ell+1}{8\pi^2}} \sum_{\lambda = \lceil \frac{|k+k'|}{2} \rceil}^{\ell} \hat{f}(\ell, k, k') C_{\ell k k'}^{2\lambda} P_{2\lambda}^{|k+k'|}(\cos\theta) \mathrm{e}^{\mathrm{i}(k'\rho - k\rho')}.$$

Substituting

$$\rho_+ = \tfrac{1}{2}(\rho + \rho'), \quad \rho_- = \tfrac{1}{2}(\rho - \rho'),$$

we define a function $g\colon \mathbb{S}^2 \times \mathbb{S}^1 \to \mathbb{C}$ by

$$\begin{aligned} g(\mathbf{u}_{\theta,\rho_-}, \mathbf{u}_{\rho_+}) &= \mathcal{M}f(\mathbf{u}_{\theta,\rho_+-\rho_-}, \mathbf{u}_{\theta,\rho_++\rho_-}) \\ &= \sum_{(\ell,k,k') \in J} \sqrt{\frac{2\ell+1}{8\pi^2}} \hat{f}(\ell, k, k') \sum_{\lambda = \lceil \frac{|k+k'|}{2} \rceil}^{\ell} C_{\ell k k'}^{2\lambda} P_{2\lambda}^{|k+k'|}(\cos\theta) \mathrm{e}^{\mathrm{i}(k+k')\rho_-} \mathrm{e}^{\mathrm{i}(k'-k)\rho_+} \\ &= \sum_{(\ell,k,k') \in J} \hat{f}(\ell, k, k') \sum_{\lambda = \lceil \frac{|k+k'|}{2} \rceil}^{\ell} \sqrt{\frac{2\ell+1}{4\lambda+1}} C_{\ell k k'}^{2\lambda} \mathcal{Y}_{2\lambda}^{k+k'}(\mathbf{u}_{\theta,\rho_-}) \frac{1}{\sqrt{2\pi}} \mathrm{e}^{\mathrm{i}(k'-k)\rho_+}. \end{aligned}$$

Since g is bounded and periodic with respect to ρ_+ and ρ_- it permits for a series expansion with respect to spherical harmonics and exponentials

$$g(\mathbf{u}_{\theta,\rho_-}, \mathbf{u}_{\rho_+}) = \sum_{(\tau,k_+)\in I} \sum_{k_-\in\mathbb{Z}} \hat{g}(\tau, k_+, k_-) \mathcal{Y}_\tau^{k_+}(\mathbf{u}_{\theta,\rho_-}) \frac{1}{\sqrt{2\pi}} \mathrm{e}^{ik_-\rho_+}$$

with Fourier coefficients $\hat{g}(\tau, k_+, k_-) \in \ell^2(I \times \mathbb{Z})$ given by

$$\hat{g}(\tau, k_+, k_-) = \int_0^{2\pi} \int_0^{2\pi} \int_0^{\pi} g(\mathbf{u}_{\theta,\rho_-}, \mathbf{u}_{\rho_+}) \overline{\mathcal{Y}_\tau^{k_+}(\mathbf{u}_{\theta,\rho_-})} \frac{1}{\sqrt{2\pi}} \mathrm{e}^{-ik_-\rho_+} \sin\theta \, \mathrm{d}\rho \, \mathrm{d}\rho' \, \mathrm{d}\theta.$$

Plugging in the definition of g and making use of the orthogonality relations of the exponentials and the spherical harmonics we observe that all integrals vanish except for those with $k_+ = k+k'$, $k_- = k' - k$ and $\tau = 2\lambda$ and we have

$$\hat{g}(\tau, k_+, k_-) = \begin{cases} \sum_{\ell=\tau/2}^{\infty} \sqrt{\frac{2\ell+1}{2\tau+1}} \hat{f}(\ell, k, k') C_{\ell k k'}^{\tau} & \tau \in 2\mathbb{N}, \\ 0 & \text{otherwise.} \end{cases}$$

Decomposing this relation into

$$\hat{h}(2\lambda, k, k') = \sum_{\ell=\lambda}^{\infty} \sqrt{\frac{2\ell+1}{4\lambda+1}} \hat{f}(\ell, k, k') C_{\ell k k'}^{2\lambda}, \quad (2\lambda, k, k') \in \tilde{J}$$

and

$$\hat{g}(\tau, k_+, k_-) = \begin{cases} \hat{h}(\tau, \frac{k_+ + k_-}{2}, \frac{k_+ - k_-}{2}) & \tau \in 2\mathbb{N}, \\ 0 & \text{otherwise,} \end{cases}$$

we finally obtain $\hat{f} = \mathcal{F}_{\mathrm{SO}(3)}^{-1} f$, $\hat{h} = \mathcal{C}\hat{f}$, $\hat{g} = \mathcal{P}\hat{h}$ and $g = \mathcal{F}_{\mathbb{S}^2} \hat{\otimes} \mathcal{F}_{\mathbb{S}^1} \hat{g}$. □

3.3 The forward problem

In this section we are going to give a discrete version of Theorem 8 and utilize it for a fast algorithm for the forward problem. To this end we restrict ourselves to sampling sets $\mathbf{u}_{\rho_m,\theta_n}, \mathbf{u}_{\rho_{m'},\theta_n} \in \mathbb{S}^2$ with equispaced angles $\rho_m = \frac{2\pi m}{M}$, $\rho_{m'} = \frac{2\pi m'}{M}$, $m, m' = 0, \ldots, M-1$, since this ensures that the set of all sums $\rho_+ = \frac{\rho_m + \rho_{m'}}{2}$ and difference angles $\rho_- = \frac{\rho_m - \rho_{m'}}{2}$ modulo 2π has the cardinality $2M - 1$.

We start by defining bandlimited analogues to the continuous operators $\mathcal{C}$ and $\mathcal{P}$. Let $\hat{\mathbf{f}} \in \mathbb{C}^{J_L}$ be the vector of Fourier coefficients of a polynomial $f \in \Pi_L(\mathrm{SO}(3))$ and

$$\tilde{J}_L = \{ (2\lambda, k, k') \in 2\mathbb{N}_0 \times \mathbb{Z} \times \mathbb{Z} \mid |k|, |k'| \le L \text{ and } |k + k'| \le 2\lambda \le 2L \}$$

the restriction of the index set $\tilde{J}$ to bandlimited function. Then we define the matrix $\mathbf{C}_L \in \mathbb{C}^{\tilde{J}_L \times J_L}$ as the restriction of the operator $\mathcal{C}$ to $\mathbb{C}^{J_L}$, i.e., by

$$\hat{\mathbf{h}} = \mathbf{C}_L \hat{\mathbf{f}}, \quad \hat{\mathbf{h}}_{2\lambda,k,k'} = \sum_{\ell=\lambda}^{L} \frac{\sqrt{2\ell+1}}{\sqrt{4\lambda+1}} C_{\ell k k'}^{2\lambda} \hat{\mathbf{f}}_{\ell,k,k'}, \quad (2\lambda, k, k') \in \tilde{J}_L.$$

Since, the matrix $\mathbf{C}_L$ is blockdiagonal with upper triangle blocks and non zero diagonal elements the matrix $\mathbf{C}_L$ is invertible. Its inverse $\mathbf{C}_L^{-1}$ is given by $\hat{\mathbf{f}} = \mathbf{C}_L^{-1}\hat{\mathbf{h}}$,

$$\hat{\mathbf{f}}_{\ell,k,k'} = \left(C^{2\ell}_{\ell,k,k'}\right)^{-1}\left(\frac{\sqrt{4\ell+1}}{\sqrt{2\ell+1}}\hat{\mathbf{h}}_{2\ell,k,k'} - \sum_{\tau=\ell+1}^{L}\frac{\sqrt{2\tau+1}}{\sqrt{4\ell+1}}C^{2\ell}_{\tau,k,k'}\hat{\mathbf{f}}_{\tau,k,k'}\right), \quad (\ell,k,k') \in J_L. \quad (22)$$

Furthermore, we define the rotation matrix $\mathbf{P}_M \in \mathbb{C}^{(2M-1)^2\times M^2}$ by $\tilde{\mathbf{g}} = \mathbf{P}\mathbf{g}$,

$$\tilde{\mathbf{g}}_{m_+,m_-} = \begin{cases}\mathbf{g}_{\frac{m_++m_-}{2},\frac{m_+-m_-}{2}}, & \text{if } m_+ + m_- \text{ is even}\\ 0, & \text{if } m_+ + m_- \text{ is odd}\end{cases},$$

$m_+ = 0,\dots,2M-1$, $m_- = 1-M,\dots,M-1$, and for $\lambda = 0,\dots,L$ the rotation matrices $\mathbf{P}_{L,\lambda} \in \mathbb{C}^{(2L-1)(2\lambda+1)\times(2L-1)^2}$ by $\hat{\mathbf{g}}_\lambda = \mathbf{P}_{L,\lambda}\hat{\mathbf{h}}_\lambda$,

$$\hat{\mathbf{g}}_{\lambda,k_+,k_-} = \begin{cases}\hat{\mathbf{h}}_{\lambda,\frac{k_++k_-}{2},\frac{k_+-k_-}{2}}, & \text{if } k_+ + k_- \text{ is even,}\\ 0, & \text{if } k_+ + k_- \text{ is odd,}\end{cases} \quad (23)$$

where $k_+ = -\lambda,\dots,\lambda$ and $k_- = -L,\dots,L$. With these definitions we have the following discrete decomposition result.

Theorem 9. *Let $f \in \Pi_L(\mathrm{SO}(3))$ be a polynomial of degree $L \in \mathbb{N}$ with Fourier coefficients $\hat{\mathbf{f}} \in \mathbb{C}^{J_L}$ and let $(\mathbf{u}_{\rho_m,\theta_n}, \mathbf{u}_{\rho_{m'},\theta_n})$, $\rho_m = \frac{2\pi m}{M}$, $\theta_n = \frac{\pi n}{N}$, $m, m' = 0,\dots,M-1$, $n = 0,\dots,N$, be a regular sampling set for the characteristic manifold $\Omega_{\mathbf{e}_3,\mathbf{e}_3}$. Then the evaluation $\mathbf{g} \in \mathbb{C}^{M\times M\times N}$ of the Funk transform $\mathbf{g}_{n,m,m'} = \mathcal{M}f(\mathbf{u}_{\rho_m,\theta_n}, \mathbf{u}_{\rho_{m'},\theta_n})$ at this sampling set can be factorized as*

$$\mathbf{g} = (\mathbf{I}_N \otimes \mathbf{P}_M)^H(\mathbf{F}_{\mathbb{S}^2,2L} \otimes \mathbf{F}_{\mathbb{S}^1,2L})\bigoplus_{\lambda=0}^{2L}\mathbf{P}_{L,\lambda}\,\mathbf{C}_L\,\hat{\mathbf{f}},$$

where $\mathbf{F}^H_{\mathbb{S}^2,2L}$ is the discrete spherical Fourier transform at nodes $\mathbf{u}_{\rho_m,\theta_n}$, $m = 0,\dots,M-1$, $n = 0,\dots,N$.

In particular, the factorization allows for an implementation as shown in Algorithm 1 which has for $\mathcal{O}(M) = \mathcal{O}(N) = \mathcal{O}(L)$ the numerical complexity $\mathcal{O}(L^4)$.

Proof. The validity of the decomposition follows directly from the proof of Theorem 8. For the numerical complexity we note that direct evaluation of the matrix vector product $\mathbf{C}_L\,\hat{\mathbf{f}}$ involves $\mathcal{O}(L^4)$ operations. The multiplication with the permutation matrices $\mathbf{P}_{L,\lambda}$, $\lambda = 1,\dots,L,\lambda$, has the numerical complexity $\mathcal{O}(L^3)$. For the Fourier transforms on $\mathbb{S}^1$ we have to compute $|I_L|$ times an FFT which gives the numerical complexity $\mathcal{O}(L^3\ln(L))$ where we have assumed that $\mathcal{O}(M) = \mathcal{O}(L)$. For the spherical Fourier transform we utilize the nonequispaced fast spherical Fourier transform (NFSFT) as described in [16] and implemented in [17]. The corresponding numerical complexity is $\mathcal{O}(L^3\ln^2(L))$ given that $\mathcal{O}(M) = \mathcal{O}(N) = \mathcal{O}(L)$. The final permutation has the numerical complexity $\mathcal{O}(NM^2)$. □

The numerical complexity $\mathcal{O}(L^4)$ of Algorithm 1 compares favorable to the numerical complexity $\mathcal{O}(L^6)$ of a direct implementation.

Algorithm 1: Fast Funk transform

input : $\rho_m = \frac{2\pi m}{M}, m = 0, \ldots, M-1$
$\rho_{m'} = \frac{2\pi m'}{M}, m = 0, \ldots, M-1$
$\theta_n = \frac{\pi n}{N}, n = 0, \ldots, N$
$\hat{f}(\ell, k, k'), \ell = 0, \ldots, L, k, k' = -\ell, \ldots, \ell$

output: $g(n, m, m') = \mathcal{M}f(\mathbf{u}_{\rho_m,\theta_n}, \mathbf{u}_{\rho_{m'},\theta_n})$

Step 1: polynomial transform - complexity $\mathcal{O}(L^4)$

for $\lambda = 0$ **to** L **do** **for** $k, k' = -L$ **to** L **do**

$$\hat{h}(\lambda, k, k') \leftarrow \sum_{\ell=\lambda}^{L} \frac{\sqrt{2\ell+1}}{\sqrt{4\lambda+1}} C_{\ell k k'}^{2\lambda} \hat{f}(\ell, k, k')$$

end

Step 2: rotation of the Fourier coefficients - complexity $\mathcal{O}(L^3)$

for $\lambda = 0$ **to** L **do**

for $k_+ = -2\lambda$ **to** 2λ **do** **for** $k_- = -2L + |k_+|$ **to** $2L - |k_+|$ **do**

$\hat{g}(2\lambda, k_+, k_-) \leftarrow \hat{h}(\lambda, \frac{k_+ - k_-}{2}, \frac{k_+ + k_-}{2})$

end

end

Step 3: FFTs with respect to k_- *- complexity* $\mathcal{O}(L^2(M + L\log L))$

for $\lambda = 0$ **to** L **do** **for** $k_+ = -2\lambda$ **to** 2λ **do**

for $m_+ = 0$ **to** $2M - 2$ **do**

$$\hat{\hat{g}}(2\lambda, k_+, m_+) \leftarrow \frac{1}{\sqrt{2\pi}} \sum_{k_-=-2L}^{2L} \hat{g}(2\lambda, k_+, k_-)\, \mathrm{e}^{2\pi \mathrm{i} \frac{k_- m_+}{2M}}$$

end

end

Step 4: NFSFTs with respect to (λ, k_+) *- complexity* $\mathcal{O}(M(MN + L^2 \log^2 L))$

for $m_+ = 0$ **to** $2M - 2$ **do**

for $n = 0$ **to** N **do** **for** $m_- = 1 - M$ **to** $M - 1$ **do**

$$\tilde{g}(n, m_-, m_+) \leftarrow \sum_{(\lambda, k_+) \in I_{2L}} \hat{\hat{g}}(\lambda, k_+, m_+) \mathcal{Y}_{\lambda}^{k_+}(\mathbf{u}_{\theta_n, \frac{2\pi m_-}{2M}})$$

end

end

Step 5: rotation of the function values - complexity $\mathcal{O}(M^2 N)$

for $n = 0$ **to** N **do** **for** $m, m' = 0$ **to** $M - 1$ **do**

$g(n, m, m') \leftarrow \tilde{g}(n, m + m', m - m')$

end

Numerical Experiments. Next we want to perform some numerical experiments to illustrate the performance of Algorithm 1 with respect to accuracy. All test have been run on an Intel™ I7-970 computer with 24 GB main memory, SuSe-Linux (64 bit), using double precision arithmetic. The algorithms were implemented in MATLAB using the MEX (MATLAB to C) interface of the NFFT 3.0.2, cf. [15, 17], libraries together with the FFTW 3.3.3, cf. [8]. Whenever involved we used the NFFT with oversampling factor $\rho = 2$, precomputed Kaiser-Bessel functions and NFFT-intern cut-off parameter $m = 10$. A critical part of the presented algorithm is the computation of the Wigner–3j symbols which are needed for the Clebsch Gordon coefficients. In our experiments we used the MATLAB toolbox SHTOOLS [44] which implements two algorithms described in [21, 36] for the computation of the Wigner–3j symbols. It should be noted that the Wigner-3j symbols are not computed exactly up to machine precision, but contain errors up to 10^{-4}. With the following test we try to illustrate the impact of these errors to the accuracy of our forward algorithm.

For our tests we start with a polynomial of degree L given by its Fourier expansion

$$f(\mathbf{R}) = \sum_{(\ell,k,k')\in J_L} \hat{f}(\ell,k,k')\sqrt{2\ell+1}D_\ell^{k,k'}(\mathbf{R})$$

with random Fourier coefficients $|\hat{f}(\ell,k,k')| < 1$. In practical applications we would apply the adjoined NFSOFT, cf. [30], and a quadrature rule to determine the Fourier coefficients from a certain sampling of the function f.

In order to estimate the accuracy of our algorithm we fix a sampling set of nodes $(\mathbf{u}_{\theta_n,\rho_m}, \mathbf{u}_{\theta_n,\rho_{m'}}) \in \Omega_{\mathbf{e}_3,\mathbf{e}_3}$, $n = 0,\ldots,N$, $m, m' = 0,\ldots,M-1$ and compute

$$g^{\text{direct}}_{n,m,m'} = \sum_{(\ell,k,k')\in J_L} \hat{f}(\ell,k,k')\frac{4\pi}{\sqrt{2\ell+1}}\mathcal{Y}_\ell^{k'}(\mathbf{u}_{\theta_n,\rho_m})\overline{\mathcal{Y}_\ell^{k}(\mathbf{u}_{\theta_n,\rho_{m'}})} \tag{24}$$

by directly evaluating the sum (24) and $g^{\text{fast}}_{n,m,m'}$, $n = 0,\ldots,N$, $m, m' = 0,\ldots,M-1$, by applying Algorithm 1. As a measure for the accuracy we consider the relative maximum error

$$\varepsilon = \frac{\max_{n,m,m'}\left|g^{\text{fast}}_{n,m,m'} - g^{\text{exact}}_{n,m,m'}\right|}{\max_{n,m,m'}\left|g^{\text{exact}}_{n,m,m'}\right|}.$$

Figure 1 displays the relative maximum error ε in dependency of the bandwidth L. We observe that the relative error increases moderately with the bandwidth.

3.4 The inverse problem

In this section we are concerned with the inversion of the function f from its Funk transform $\mathcal{M}f$ sampled at the three dimensional submanifold $\Omega_{e_3,e_3} \subset \mathbb{S}^2 \times \mathbb{S}^2$. More precisely, we consider a sampling set of nodes $(\boldsymbol{\xi}_{m,n}, \boldsymbol{\eta}_{m',n}) \in \Omega_{\mathbf{e}_3,\mathbf{e}_3}$, $m, m' = 0,\ldots,M-1$, $n = 0,\ldots,N$, that allows for a quadrature rule for polynomials on $\mathbb{S}^2 \times \mathbb{S}^1$ up to degree $2L$ and aim at the recovery of the Fourier coefficients $\hat{f}(\ell,k,k')$, $(\ell,k,k') \in J_L$ of a bandlimited function

$$f(\mathbf{R}) = \sum_{(\ell,k,k')\in J_L} \hat{f}(\ell,k,k')\sqrt{2\ell+1}D_\ell^{k,k'}(\mathbf{R}) \tag{25}$$

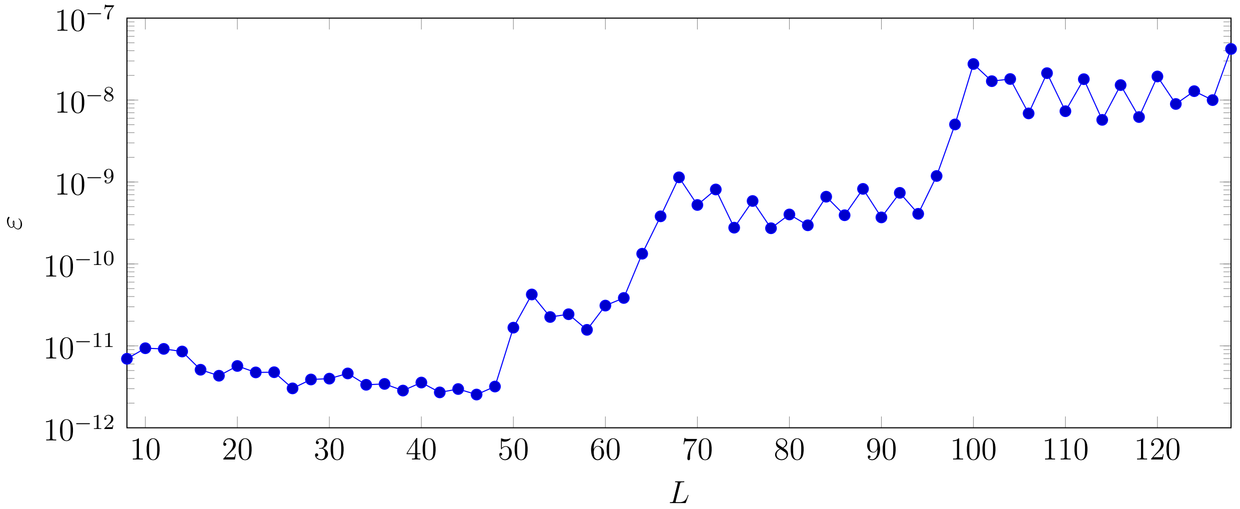

Figure 1: The accuracy of the forward Algorithm 1 in dependency of the bandwidth.

given function values $\mathbf{g} \in \mathbb{C}^{(N+1)\times M\times M}$, $g_{n,m,m'} = \mathcal{M}f(\boldsymbol{\xi}_{m,n}, \boldsymbol{\eta}_{m',n})$, $m, m' = 0, \dots, M-1$, $n = 0, \dots, M$, of the Funk transform of f.

We have the following exact reconstruction formula for bandlimited functions.

Theorem 10. *Let nodes $\theta_n \in [-1,1]$ and weights $\omega_n \in \mathbb{R}$, $n = 0, \dots, N$, be a quadrature rule on $[-1,1]$ which is exact for polynomials up to degree $4L+1$. Let, furthermore, $\rho_m = \frac{2\pi m}{M}$, $m = 0, \dots, M-1$, $M \geq L+1$, be equispaced quadrature nodes on the circle $\mathbb{S}^1$ which allow for the exact integration of polynomials up to degree $4L+1$. Then any bandlimited function $f \in \Pi_L(\mathrm{SO}(3))$ can be uniquely reconstructed from its Funk transform $\mathcal{M}f$ sampled at nodes $(\mathbf{u}_{\theta_n,\rho_m}, \mathbf{u}_{\theta_n,\rho_{m'}}) \in \Omega_{\mathbf{e}_3,\mathbf{e}_3}$, i.e., from values*

$$\mathbf{g}_{m,m',n} = \mathcal{M}f(\mathbf{u}_{\rho_m,\theta_n}, \mathbf{u}_{\rho_{m'},\theta_n}), \quad n = 0\dots, N,\ m, m' = 0, \dots, M-1.$$

The vector of Fourier coefficients $\hat{\mathbf{f}} \in \mathbb{C}^{|\mathcal{J}_L|}$ is given by

$$\hat{\mathbf{f}} = \mathbf{C}_L^{-1} \bigoplus_{\lambda=0}^{L} \mathbf{P}_{L,\lambda}^H \left(\mathbf{F}_{\mathbb{S}^2,2L}^H \otimes \mathbf{F}_{\mathbb{S}^1,2L}^H\right) (\mathbf{I}_N \otimes \mathbf{P}_M) \mathbf{W}\mathbf{g},$$

where $\mathbf{F}_{\mathbb{S}^2,2L}^H$ is the adjoined discrete spherical Fourier transform at nodes $\mathbf{u}_{\rho_m,\theta_n}$, $m = 0, \dots, M-1$, $n = 0, \dots, N$, $F_{\mathbb{S}^1,2L}^H$ is the adjoined one dimensional discrete Fourier transform and $\mathbf{W} \in \mathbb{C}^{(N+1)M^2\times(N+1)M^2}$ is the diagonal matrix that multiplies with the quadrature weights, i.e, has diagonal entries $W_{mm'n,mm'n} = \omega_n$.

More explicitly, the Fourier coefficients of f are given by

$$\hat{f}(\ell,k,k') = \left(C_{\ell,k,k'}^{2\ell}\right)^{-1} \left(\frac{\sqrt{4\ell+1}}{\sqrt{2\ell+1}} \hat{h}(2\ell,k,k') - \sum_{\tau=\ell+1}^{L} \frac{\sqrt{2\tau+1}}{\sqrt{4\ell+1}} C_{\tau,k,k'}^{2\ell} \hat{f}(\tau,k,k')\right)$$

with coefficients $\hat{h}(2\lambda, k, k')$, $\lambda = 0, \ldots, L$, $k, k' = -L, \ldots, L$, *satisfying*

$$\hat{h}(2\lambda, k, k') = \sum_{n=0}^{L} \sum_{m_+=0}^{4L-2} \sum_{m_-=-2L+1}^{2L-1} \frac{\omega_n}{M^2} \mathcal{M} f(\mathbf{u}_{\rho_{m_+ + m_-}, \theta_n}, \mathbf{u}_{\rho_{m_+ - m_-}, \theta_n}) \mathrm{e}^{\mathrm{i}\pi \frac{k_- m_+}{L}} \mathcal{Y}_{2\lambda}^{k_+}(\mathbf{u}_{\frac{2\pi m_-}{M}, \theta_n}).$$

Proof. By Theorem 9 we have

$$\mathcal{M} f(\mathbf{u}_{\rho,\theta}, \mathbf{u}_{\rho',\theta}) = \sum_{(2\lambda,k,k') \in \tilde{J}_L} \sqrt{\frac{4\lambda+1}{8\pi^2}} \hat{h}(2\lambda, k, k') \mathrm{e}^{\mathrm{i}(k'\rho - k\rho')} P_{2\lambda}^{|k+k'|}(\cos\theta)$$

with Fourier coefficients

$$\hat{h}(2\lambda, k, k') = \sum_{\ell=\lambda}^{L} \frac{\sqrt{2\ell+1}}{\sqrt{4\lambda+1}} C_{\ell k k'}^{2\lambda} \hat{f}(\ell, k, k'), \quad (2\lambda, k, k') \in \tilde{J}_L,$$

satisfying

$$\hat{h}(2\lambda, k, k') = \int_0^{2\pi} \int_0^{2\pi} \int_0^{\pi} M f(\mathbf{u}_{\rho,\theta}, \mathbf{u}_{\rho',\theta}) \sqrt{\frac{4\lambda+1}{8\pi^2}} \mathrm{e}^{\mathrm{i}(k\rho' - k'\rho)} P_{2\lambda}^{|k+k'|}(\cos\theta) \sin\theta \, \mathrm{d}\theta \, \mathrm{d}\rho \, \mathrm{d}\rho'.$$

Given that the quadrature nodes θ_n with quadrature weights ω_n, $n = 0, \ldots, N$ are exact up to degree $4L+1$ with respect to the weight $\cos\theta$ we can replace the integral for all $(2\lambda, k, k') \in \tilde{J}_L$ by the sum

$$\begin{aligned}
\hat{h}(2\lambda, k, k') &= \sum_{m,m'=0}^{M-1} \sum_{n=0}^{N} \frac{\omega_n}{M^2} \mathcal{M} f(\mathbf{u}_{\theta_n, \rho_m}, \mathbf{u}_{\theta_n, \rho_{m'}}) \sqrt{\frac{4\lambda+1}{8\pi^2}} \mathrm{e}^{\mathrm{i}(k\rho_{m',n} - k'\rho_{m,n})} P_{2\lambda}^{|k+k'|}(\cos\theta_n) \\
&= \sum_{m,m'=0}^{M-1} \sum_{n=0}^{N} \frac{\omega_n}{M^2} g_{n,m,m'} \sqrt{\frac{4\lambda+1}{8\pi^2}} \mathrm{e}^{2\pi\mathrm{i} \frac{km' - k'm}{M}} P_{2\lambda}^{|k+k'|}(\cos\theta_n).
\end{aligned}$$

Substituting

$$m_+ = m + m', \quad m_- = m - m', \quad k_+ = k' + k, \quad k_- = k' - k,$$

i.e., $k_+ m_- - k_- m_+ = 2k'm - 2km'$ and defining $\tilde{\mathbf{g}} \in \mathbb{C}^{(N+1)\times(2M-1)\times(2M-1)}$ by

$$\tilde{g}_{n,m+m',m-m'} = g_{n,m,m'}, \quad n = 0, \ldots, N, \ m, m' = 0, \ldots, M-1,$$

we arrive for all $(2\lambda, k_+) \in I_{2L}$ and $k_- = -2L \ldots 2L$ at

$$\begin{aligned}
\hat{h}(2\lambda, k, k') &= \sum_{n=0}^{N} \sum_{m_+=0}^{2M-2} \sum_{m_-=1-M}^{M-1} \frac{\omega_n}{M^2} \tilde{g}_{n,m_+,m_-} \sqrt{\frac{4\lambda+1}{8\pi^2}} \mathrm{e}^{-2\pi i \frac{k_+ m_- - k_- m_+}{2M}} P_{2\lambda}^{|k_+|}(\cos\theta_n) \\
&= \sum_{n=0}^{N} \sum_{m_+=0}^{2M-1} \sum_{m_-=1-M}^{M-1} \frac{\omega_n}{M^2} \tilde{g}_{n,m_+,m_-} \frac{1}{\sqrt{2\pi}} \mathrm{e}^{2\pi\mathrm{i} \frac{k_- m_+}{2M}} \overline{\mathcal{Y}_{2\lambda}^{k_+}(\mathbf{u}_{\theta_n, \frac{2\pi m_-}{2M}})}.
\end{aligned}$$

□

Although Theorem 10 suggests a promising Algorithm 2 for the inversion of the restricted Funk transform it is not applicable in practice. This is due to the extremely ill conditioned matrices $\mathbf{C}_L$, $L = 0, 1, \ldots$. Their condition increases exponentially with L, c.f. Table 1.

Algorithm 2: Quadrature based inversion

input : $g(n, m, m'), \quad n = 0, \ldots, N, \ m, m' = 0, \ldots, M-1$

output: $\hat{f}(\ell, k, k'), \quad (\ell, k, k') \in J_L$

Step 1: rotation of the function values - complexity $\mathcal{O}(M^2 N)$

for $n = 0$ **to** N **do** **for** $m, m' = 0$ **to** $M-1$ **do**

$\tilde{g}(m + m', m - m', n) \leftarrow g(n, m, m')$

end

Step 2: FFTs with respect to m_+ *- complexity* $\mathcal{O}(MN(M + L\log L))$

for $n = 0$ **to** N **do** **for** $m_- = -M+1$ **to** $M-1$ **do**

for $k_- = -2L$ **to** $2L$ **do**

$$\hat{\tilde{g}}(k_-, m_-, n) \leftarrow \frac{1}{\sqrt{2\pi}} \sum_{m_+=0}^{2M-1} \tilde{g}(m_+, m_-, n) \mathrm{e}^{2\pi \mathrm{i} \frac{m_+ k_-}{2M}}$$

end

end

Step 3: adjoined NFSFTs with respect to (n, m_-) *- complexity* $\mathcal{O}(M(MN + L^2 \log^2 L))$

for $k_- = -L$ **to** L **do** **for** $(2\lambda, k_+) \in I_{2L}$ **do**

$$\hat{g}(\lambda, k_+, k_-) \leftarrow \sum_{n=0}^{N} \sum_{m_-=-M+1}^{M-1} \frac{\omega_n}{M^2} \hat{\tilde{g}}(n, m_-, k_-) \overline{\mathcal{Y}_{2\lambda}^{k_+}(\mathbf{u}_{\theta_n, \frac{2\pi m_-}{2M}})}$$

end

Step 4: rotation of the Fourier coefficients - complexity $\mathcal{O}(L^3)$

for $\ell = L$ **to** 0 **do** **for** $k, k' = -\ell$ **to** ℓ **do**

$\hat{h}(\ell, k, k') \leftarrow \hat{g}(\ell, k + k', k - k')$

end

Step 5: inverse polynomial transform - complexity $\mathcal{O}(L^4)$

for $\ell = L$ **to** 0 **do** **for** $k, k' = -\ell$ **to** ℓ **do**

$$\hat{f}(\ell, k, k') \leftarrow \left(C_{\ell,k,k'}^{2\ell}\right)^{-1} \left(\sqrt{\frac{4\ell+1}{2\ell+1}} \hat{h}(\ell, k, k') - \sum_{\lambda=\ell+1}^{L} \sqrt{\frac{2\lambda+1}{2\ell+1}} C_{\lambda,k,k'}^{2\ell} \hat{f}(\lambda, k, k') \right)$$

end

L	$\mathrm{cond}(\mathbf{C}_L)$
8	10^4
16	10^9
32	10^{20}
64	10^{33}
128	10^{55}

Table 1: The approximate condition of the matrix $\mathbf{C}_L$ in dependency of the bandwidth L.

3.5 Iterative Reconstruction

Since the quadrature based approach failed gloriously in the last section we focus on iterative reconstruction by means of the least squares problem

$$\sum_{n=0}^{N} \omega_n \sum_{m,m'=0}^{M-1} \left| \mathcal{M} f(\mathbf{u}_{\theta_n,\rho_m}, \mathbf{u}_{\theta_n,\rho_{m'}}) - g_{n,m,m'} \right|^2 + \lambda \left\| \triangle f \right\|_2^2 \to \min, \tag{26}$$

where $(g_{n,m,m'}, \mathbf{u}_{\theta_n,\rho_m}, \mathbf{u}_{\theta_n,\rho_{m'}})$, $m, m' = 1, \ldots, M$, $N = 1, \ldots, N$, is a sampling as defined in Theorem 10 and $\lambda \left\| \triangle f \right\|_2^2$ is some regularization term. In contrast to the quadrature based approach we are now more free to set the weights ω_n. More precisely, we do not have to set them as the quadrature weights with respect to the weighting function $\sin\theta$, i.e., for the manifold $\mathbb{S}^2 \times \mathbb{S}^1$, but we can choose them as quadrature weights with respect to the manifold $\Omega_{\mathbf{e}_3,\mathbf{e}_3} \subset \mathbb{S}^2 \times \mathbb{S}^2$. A further advantage of this approach is that we can effectively apply oversampling as regularization.

Let us introduce the matrix $\mathbf{M} \in \mathbb{C}^{M^2 N \times |J_L|}$, c.f. Theorem 9,

$$\mathbf{M} = (\mathbf{I}_N \otimes \mathbf{P}_M)^H (\mathbf{F}_{\mathbb{S}^2,2L} \otimes \mathbf{F}_{\mathbb{S}^1,2L}) \bigoplus_{\lambda=0}^{2L} \mathbf{P}_{L,\lambda}\, \mathbf{C}_L,$$

the diagonal matrix $\mathbf{W} \in \mathbb{R}^{M^2 N \times M^2 N}$ containing the weights $W_{mm'n,mm'n} = \omega_{mm'n}$, $m, m' = 1, \ldots, M$, $N = 1, \ldots, N$ and the diagonal matrix $\mathbf{U} \in \mathbb{R}^{|J_L| \times |J_L|}$, $U_{(\ell,k,k'),(\ell,k,k')} = \ell(\ell+1)$ representing the Laplace operator in Fourier space. Then the least squares problem (26) for a vector $\mathbf{g} \in \mathbb{C}^{M^2 N}$ with entries $g_{n,m,m'} \approx \mathcal{M} f(\mathbf{u}_{\theta_n,\rho_m}, \mathbf{u}_{\theta_n,\rho_{m'}})$ and a polynomial $f \colon \mathrm{SO}(3) \to \mathbb{C}$ of degree L represented by its vector $\hat{\mathbf{f}} \in \mathbb{C}^{|J_L|}$ of Fourier coefficients $\hat{f}_{\ell,k,k'} = \hat{f}(\ell,k,k')$ becomes

$$\|\mathbf{W}^{1/2}(\mathbf{M}\hat{\mathbf{f}} - \mathbf{g})\|_2^2 + \lambda \hat{\mathbf{f}}^H \mathbf{U} \hat{\mathbf{f}} \to \min$$

which is equivalent to the normal equation

$$(\mathbf{M}^H \mathbf{W} \mathbf{M} + \lambda \mathbf{U})\hat{\mathbf{f}} = \mathbf{M}^H \mathbf{W} \mathbf{g}. \tag{27}$$

The normal equation (27) can be effectively solved by the conjugated gradient normal residual (CGNR) algorithm, cf. e.g. [33], the only ingredients of which are fast algorithms for the direct transform $\mathbf{W}^{1/2}\mathbf{M} + \lambda\mathbf{U}^{1/2}$ and for the corresponding adjoined transform. Let us assume $\mathcal{O}(L) = \mathcal{O}(M) = \mathcal{O}(N)$. Then an algorithm with numerical complexity $\mathcal{O}(L^4)$ for the direct transform can be derived from Algorithm 1 by additionally applying the diagonal matrices $\mathbf{W}^{\frac{1}{2}}$ and $\mathbf{U}^{\frac{1}{2}}$. Similarly, an algorithm for the adjoined transform with the same numerical complexity can be derived from Algorithm 2 by replacing the multiplication with the inverse of $\mathbf{C}_L$ with multiplications with its adjoined.

Numercial Experiments. Again we want to perform some numerical experiments to illustrate the suitability of the iterative approach for the inverse problem.

In a first experiment we assume f to be a polynomial of degree $L = 0, \ldots, 64$, with randomly chosen Fourier coefficients. Furthermore, we fix the number of sampling nodes to $N = 192$ and $M = 256$. This results in a total of $12\,582\,912$ sampling nodes while the dimension of the polynomial space is at maximum $366\,145$, i.e., we use a large oversampling factor of 30 as regularization which allows us to discard the regularization term, i.e, we set $\lambda = 0$. As sampling nodes we consider Clenshaw Curtis nodes $(\mathbf{u}_{\rho_m,\theta_n}, \mathbf{u}_{\rho_{m'},\theta_n})$, cf. (7), with weights ω_n^2 being the square of the Clenshaw Curtis weights do reflect the geometry of the manifold $\Omega_{\mathbf{e}_3,\mathbf{e}_3}$.

Restricting the number of iterations to 128 we compute Fourier coefficients $\hat{f}_{\text{rec}}(\ell, k, k')$, $(\ell, k, k') \in J_L$ and the relative error

$$\varepsilon(L) = \frac{\sum_{(\ell,k,k')\in J_L} \left|\hat{f}(\ell, k, k') - \hat{f}_{\text{rec}}(\ell, k, k')\right|^2}{\sum_{(\ell,k,k')\in J_L} \left|\hat{f}(\ell, k, k')\right|^2}.$$

The relative error with respect to the polynomial degree L is plotted in Figure 2.

In a second experiment we simulate a real live experiment by choosing a nonbandlimited function $f \in C(\mathrm{SO}(3))$ and analyzing the reconstruction error with respect to the polynomial degree and the number of sampling points. To this end, we consider the Abel-Poisson kernel (cf. [40]),

$$\psi_\kappa(\mathbf{R}) = \frac{1-\kappa^2}{(1+2\kappa t+\kappa^2)^2} + \frac{1-\kappa^2}{(1-2\kappa t+\kappa^2)^2} = \sum_{\ell=0}^{\infty} \kappa^{2\ell}(2\ell+1)\mathcal{U}_{2\ell}(t), \tag{28}$$

where $t = \frac{1}{2}(\operatorname{Tr}\mathbf{R} - 1)$, $\kappa \in (0, 1)$ is a free parameter influencing the sharpness of the Abel-Poisson kernel and $\mathcal{U}_{2\ell}$ denotes the Chebyshev polynomial of second type and order 2ℓ. For the test function $f\colon \mathrm{SO}(3) \to \mathbb{R}$ we randomly chose $K = 5$ rotations $\mathbf{R}_k \in \mathrm{SO}(3)$, kernel parameters $\kappa_k \in (0, 1)$ and coefficients $c_k \in [-1, 1]$; and set f to

$$f(\mathbf{R}) = \sum_{k=1}^{5} c_k \psi_{\kappa_k}(\mathbf{R}\mathbf{R}_k^{-1}). \tag{29}$$

Since the Funk transform of the Abel Poisson kernel is given by (cf. [40])

$$\mathcal{M}\psi_\kappa(\boldsymbol{\xi}, \boldsymbol{\eta}) = \frac{1-\kappa^4}{(1-2\kappa^2(\boldsymbol{\xi}\cdot\boldsymbol{\eta})+\kappa^4)^{3/2}}, \tag{30}$$

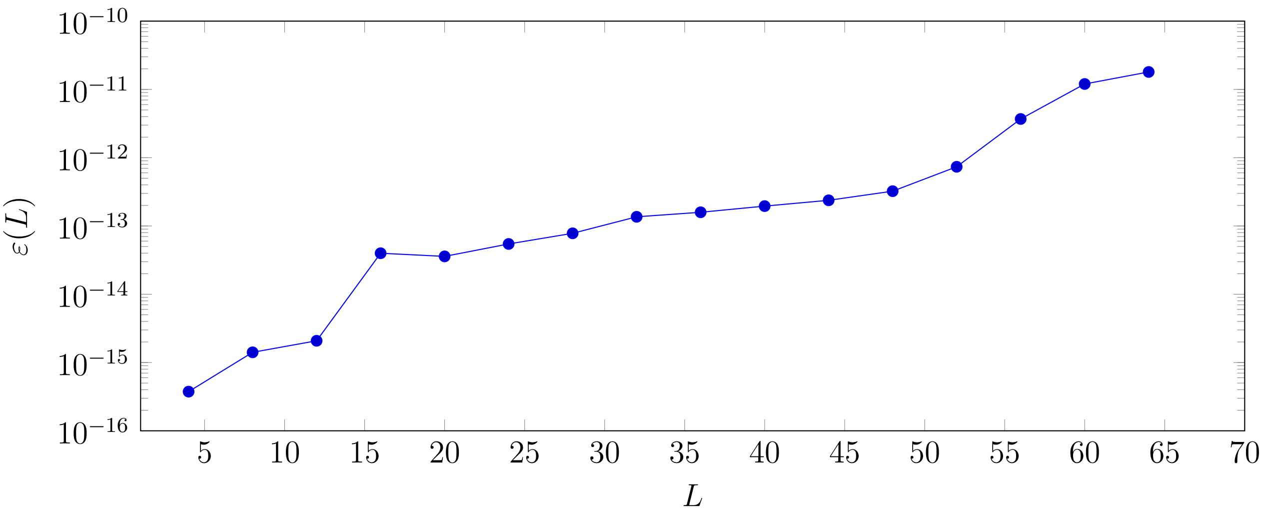

Figure 2: The relative error $\varepsilon(L)$ between the reconstructed Fourier coefficients $\hat{f}_{\text{rec}}(\ell, k, k')$ and the given Fourier coefficients $\hat{f}(\ell, k, k')$ of a polynomial f of order L given a sampling $g_{n,m,m'} = \mathcal{M}f(\mathbf{u}_{\theta_n,\rho_m}, \mathbf{u}_{\theta_n,\rho_{m'}})$, $m, m' = 1, \ldots, 256$, $N = 1, \ldots, 192$.

we can compute the Funk transform $\mathcal{M}f$ of f at Clenshaw–Curties nodes $(\mathbf{u}_{n,m}, \mathbf{u}_{n,m'})$,

$$g_{n,m,m'} = \mathcal{M}f(\mathbf{u}_{n,m}, \mathbf{u}_{n,m'}), \quad m, m' = 0, \ldots, M-1, n = 0, \ldots, N, \tag{31}$$

exactly. As in practical experiments diffraction data are corrupted by Poisson noise we simulate Poisson distributed sample values

$$\tilde{g}_{n,m,m'} = \alpha^{-1}\text{Pois}(\alpha\, g_{n,m,m'}),$$

where α controls the standard deviation of the Poisson distribution which can be interpreted as the amount of detected particles. It should be stressed that in contrast to real world diffraction data we did not restrict the data to the even part by taking means $\frac{1}{2}\big(\mathcal{M}f(\mathbf{u}_{n,m}, \mathbf{u}_{n,m'}) + \mathcal{M}f(-\mathbf{u}_{n,m}, \mathbf{u}_{n,m'})\big)$.

In contrast to the first experiment we alter the polynomial degree of the reconstruction and the number of sampling points simultaneously. More specifically, we choose $M = N = 4L$. Performing $4L$ iterations of the CGNR algorithm we obtain Fourier coefficients $\hat{f}_{\text{rec}}(\ell, k, k')$, $(\ell, k, k') \in J_L$. Utilizing the fast nonequispaced Fourier transform on the rotation group, cf. [30], we evaluate the reconstructed polynomial

$$f_{\text{rec}} = \sum_{(\ell,k,k') \in J_L} \sqrt{\frac{2\ell+1}{8\pi^2}}\, \hat{f}_{\text{rec}}(\ell, k, k') D_\ell^{k,k'}$$

at about $1\,000\,000$ approximately equispaced distributed rotations $\mathbf{R}_i \in \mathrm{SO}(3)$ and compare these values $f_{\text{rec}}(\mathbf{R}_i)$ with the corresponding values $f(\mathbf{R}_i)$ of test function f which can be computed directly by formula (28) and (29). The maximum error between these discrete function

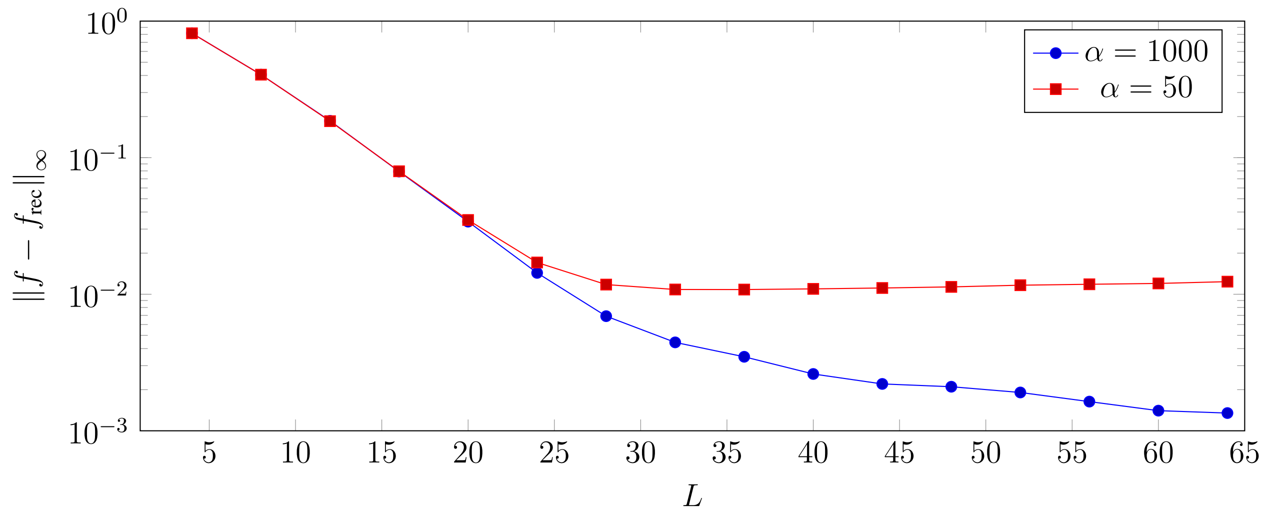

Figure 3: The approximate maximum error $\|f - f_{\text{rec}}\|_\infty$ between a nonbandlimited test function f and its reconstruction f_{rec} computed by the CGNR based algorithm given a sampling of the Funk transform of f at $(4L)^3$ sampling points with Poisson noise.

evaluations serves us as an approximation of the maximum error $\|f_{\text{rec}} - f\|_\infty$ between the test function f and its polynomial reconstruction f_{rec}. Figure 3 displays this approximation of the maximum error $\|f_{\text{rec}} - f\|_\infty$ with respect to the polynomial degree L. The numerical results indicate the applicability of the CGNR based algorithm even for noisy data.

References

[1] J. V. Bernier, M. P. Miller, and D. E. Boyce. A novel optimization-based pole-figure inversion method: comparison with WIMV and maximum entropy methods. *J. Appl. Cryst.*, 39:697 – 713, 2006.

[2] S. Bernstein and S. Ebert. Wavelets on S3 and SO(3) – their construction, relation to each other and Radon transform of wavelets on SO(3). *Math. Methods Appl. Sci.*, 33:1895 – 1909, 2010.

[3] S. Bernstein, S. Ebert, and I. Pesenson. Generalized splines for Radon transform on compact Lie groups with applications to crystallography. *J. Fourier Anal. Appl.*, 19(1):140 – 166, 2013.

[4] H. J. Bunge. Zur Darstellung allgemeiner Texturen. *Z. Metallk.*, 56:872 – 874, 1965.

[5] H. J. Bunge. *Texture Analysis in Material Science*. Butterworths, 1982.

[6] H. J. Bunge and C. Esling. The harmonic method. In H. R. Wenk, editor, *Prefered Orientations in Deformed Metals and Rocks - An Introduction to Modern Texture Analysis*, pages 109 – 122. Academic Press, Orlando, 1985.

[7] P. Cerejeiras, M. Ferreira, U. Kähler, and G. Teschke. Inversion of the noisy radon transform on SO(3) by Gabor frames and sparse recovery principles. *Appl. Comput. Harmon. Anal.*, 31:325 – 345, 2011.

[8] M. Frigo and S. G. Johnson. FFTW, C subroutine library. `http://www.fftw.org`, 2009.

[9] S. Helgason. *The Radon Transform*. Birkhäuser, 2nd edition, 1999.

[10] K. Helming and T. Eschner. A new approach to texture analysis of multiphase materials using a texture component model. *Cryst. Res. Technol.*, 25:K203 – K208, 1990.

[11] R. Hielscher, D. Potts, J. Prestin, H. Schaeben, and M. Schmalz. The Radon transform on $SO(3)$: A Fourier slice theorem and numerical inversion. *Inverse Problems*, 24:025011, 2008.

[12] R. Hielscher and H. Schaeben. A novel pole figure inversion method: specification of the *MTEX* algorithm. *Journal of Applied Crystallography*, 41(6):1024–1037, 2008.

[13] J. Imhof. An iteration procedure in the texture analysis. *Phys. Stat. Sol. (a)*, 75:K187 – K189, 1983.

[14] F. John. The ultrahyperbolic differential equation with four independent variables. *Duke Math. J.*, 4(2):300 – 322, 1938.

[15] J. Keiner, S. Kunis, and D. Potts. NFFT 3.0, C subroutine library. `http://www.tu-chemnitz.de/~potts/nfft`.

[16] J. Keiner, S. Kunis, and D. Potts. Efficient reconstruction of functions on the sphere from scattered data. In *Proceedings of ICIAM*, 2007.

[17] J. Keiner, S. Kunis, and D. Potts. Using NFFT3 - a software library for various nonequispaced fast Fourier transforms. *ACM Trans. Math. Software*, 36:Article 19, 1 – 30, 2009.

[18] J. Keiner and D. Potts. Fast evaluation of quadrature formulae on the sphere. *Math. Comput.*, 77:397 – 419, 2008.

[19] J. Keiner and A. Vollrath. A New Algorithm for the Nonequispaced Fast Fourier Transform on the Rotation Group. *SIAM J. Sci. Comput.*, 2012. to appear.

[20] P. J. Kostelec and D. N. Rockmore. FFTs on the rotation group. *J. Fourier Anal. Appl.*, 14:145 – 179, 2008.

[21] J. Luscombe and M. Luban. Simplified recursive algorithm for wigner 3j and 6j symbols. *Phys. Rev. E*, 57:7274 – 7277, 1998.

[22] S. Matthies. On the basic elements of and practical experiences with the WIMV algoeithm – an ODF reproduction method with conditional ghost correction. In J. S. Kallend and G. Gottstein, editors, *ICOTOM8*, pages 37 – 48, Santa Fe, NM, USA, 1988. The Metallurgical Society.

[23] S. Matthies, G. Vinel, and K. Helmig. *Standard Distributions in Texture Analysis*, volume 1. Akademie-Verlag Berlin, 1987.

[24] L. Meister and H. Schaeben. A concise quaternion geometry of rotations. *MMAS*, 28:101 – 126, 2004.

[25] C. Müller. *Spherical Harmonics*. Springer, Aachen, 1966.

[26] D. I. Nikolayev and H. Schaeben. Characteristics of the ultrahyperbolic differential equation governing pole density functions. *Inverse Problems*, 15:1603 – 1619, 1999.

[27] V. P. Palamodov. Reconstruction from a sampling of circle integrals in SO(3). *Inverse Problems*, 26(9):095008, 2010.

[28] K. Pawlik. Determination of the orientation distribution function from pole figures in arbitrarily defined cells. *phys. stat. sol.*, 134:477 – 483, 1986.

[29] J. Pospiech and J. Jura. Determination of the orientation distribution function from incomplete pole figures – an example of a computer program. *Texture of Cryst. Sol.*, 3:1 – 25, 1978.

[30] D. Potts, J. Prestin, and A. Vollrath. A fast algorithm for nonequispaced Fourier transforms on the rotation group. *Numer. Algorithms*, 52:355 – 384, 2009.

[31] R. J. Roe. Description of crystallite orientation in polycrystal materials III. General solution to pole figure inversion. *J. Appl. Phys.*, 36:2024 – 2031, 1965.

[32] D. Ruer. *Methode vectorielle d'analyse de la texture*. PhD thesis, Universite de Metz, France, 1976.

[33] Y. Saad. *Iterative Methods for Sparse Linear Systems*. PWS Publ., Boston, 1st edition, 1996.

[34] T. I. Savyolova and S. F. Kourtasov. ODF restoration by orientation grid. In *ICOTOM 14, Materials Science Forum*, volume Vols. 495 – 497, pages 301 – 306, 2005.

[35] H. Schaeben. Entropy optimization in quantitative texture analysis. *J. Appl. Phys.*, 64:2236 – 2237, 1988.

[36] K. Schulten and R. G. Gordon. Exact recursive evaluation of 3j-coefficients and 6j-coefficients for quantum-mechanical coupling of angular momenta. *J. Math. Phys.*, 16:1961 – 1970, 1975.

[37] A. Vadon and J. J. Heizmann. A new program to calculate the texture vector for the vector method. In C. Esling and R. Penelle, editors, *ICOTOM9*, pages 37 – 44, Avignon, France, 1991.

[38] P. Van Houtte. The use of a quadratic form for the determination of non-negative texture functions. *Textures and Microstructures*, 6:1 – 19, 1983.

[39] D. Varshalovich, A. Moskalev, and V. Khersonskii. *Quantum Theory of Angular Momentum*. World Scientific Publishing, Singapore, 1988.

[40] K. G. v.d. Boogaart, R. Hielscher, J. Prestin, and H. Schaeben. Kernel-based methods for inversion of the radon transform on $\mathrm{SO}(3)$ and their applications to texture analysis. *J. Comput. Appl. Math.*, 199:122 – 140, 2007.

[41] N. J. Vilenkin and A. U. Klimyk. *Representation of Lie Groups and Special Functions*, volume 1. Kluwer Academic Publishers, 1991.

[42] J. Waldvogel. Fast construction of Fejer and Clenshaw-Curtis quadrature rules. *BIT*, 46:195 – 202, 2006.

[43] H. R. Wenk, H. J. Bunge, J. S. Kallend, K. Loecke, S. Matthies, J. Pospiech, and P. Van Houtte. Orientation distributions: Representation and determination. In J. S. Kallend and G. Gottstein, editors, *ICOTOM 8*, pages 17 – 30, Santa Fe, 1987.

[44] M. Wieczorek. Shtools.